NASA TN D-902

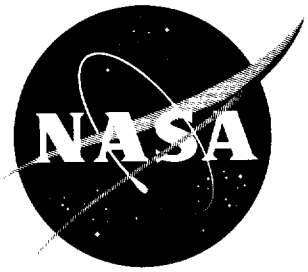

TECHNICAL NOTE

D-902

APPLICATIONS OF POWER SPECTRAL ANALYSIS METHODS TO MANEUVER LOADS OBTAINED ON JET FIGHTER AIRPLANES DURING SERVICE OPERATIONS

By John P. Mayer and Harold A. Hamer

Langley Research Center
Langley Field, Va.

NATIONAL AERONAUTICS AND SPACE ADMINISTRATION

WASHINGTON May 1961

A

NATIONAL AERONAUTICS AND SPACE ADMINISTRATION

TECHNICAL NOTE D-902

APPLICATIONS OF POWER SPECTRAL ANALYSIS METHODS TO MANEUVER LOADS OBTAINED ON JET FIGHTER AIRPLANES DURING SERVICE OPERATIONS[1]

By John P. Mayer and Harold A. Hamer

SUMMARY

Power spectral densities of normal load factor have been obtained for two service operational training flights of a Republic F-84G airplane and three service operational training flights of a North American F-86A airplane in order to indicate the load-factor frequency content and possible uses of power spectral methods in analyzing maneuver load data.

It was determined that the maneuvering load-factor time histories appeared to be described by a truncated normal distribution.

The power spectral densities obtained were relatively level at frequencies below 0.03 cycle per second and varied inversely with approximately the cube of the frequency at the higher frequencies. In general, the frequency content was very low above 0.2 cycle per second.

The load-factor peak distributions were estimated fairly well from the spectrum analysis. In addition, peak load data obtained during service operations of fighter-type airplanes with flight time totaling about 24,000 hours were examined and appeared to agree reasonably well with the type of equations obtained from spectrum peak-load distributions.

INTRODUCTION

With a view toward providing information for the appraisal of the design requirements of future airplanes, the National Advisory Committee for Aeronautics with the cooperation of the U. S. Air Force and the Bureau of Aeronautics, Department of the Navy, has been conducting a statistical study of the pilot input, the airplane motions, and the

[1]Supersedes NACA Research Memorandum L56J15 by John P. Mayer and Harold A. Hamer, 1957.

loads imposed on a number of fighter-type airplanes during military service operations. The data obtained thus far are summarized in reference 1.

The statistical treatment of the maneuver loads has been limited to the peak values of the loads and the frequency of occurrence. In the analysis of other loads associated with such random factors as gusts, buffeting, or runway roughness (for example, refs. 2 to 5), the application of power spectral analysis methods has proved valuable, especially since a number of useful theoretical relationships such as the input-output relations and the frequency of occurrence of peak loads have been established for stationary random processes. Such methods of analysis, however, have not been applied to maneuver loads. A single maneuver is clearly not a random process since it is associated with pilot intent. Nevertheless, maneuvering of a general nature (other than specific missions) over a long period of time or a collection of a great many maneuvers may acquire some of the characteristics of a random process. Therefore, it was believed that some of the relationships from the theories of spectral analysis might be used as a guide in analyzing the maneuver load data.

With this in mind, the normal load factors obtained in several flights of two jet fighter airplanes flown in regular squadron operations were analyzed by using power spectral methods. The data analyzed were obtained during the investigations reported in reference 1 and they are a portion of the results summarized in reference 1.

It is the purpose of this paper to present the power spectra obtained in order to show the frequency content of normal load factor in service operations and to determine whether other information obtainable from spectral analysis methods (such as the frequency of occurrence of peak loads) could be obtained from the maneuver load spectrum.

Power spectral densities at frequencies up to 1 cycle per second are presented for two operational flights of a Republic F-84G airplane and for three operational flights of a North American F-86A airplane. The peak loads derived from these spectra are compared with the actual peak loads. In addition, peak-load data from other service airplanes are examined and compared with the results of spectrum analysis.

SYMBOLS

a	constant used in spectrum equation
f	frequency, cps

f_B "break" frequency, cps

f_n frequency of occurrence of normal load factor

f_0 average number of normal load factor crossings per second of the zero axis with positive slope,

$$f_0^2 = \frac{\int_0^\infty f^2 \Phi(f)_{\Delta n}\, df}{\int_0^\infty \Phi(f)_{\Delta n}\, df} \quad \text{(ref. 4)}$$

f_p total number of positive normal-load-factor peaks per second,

$$f_p^2 = \frac{\int_0^\infty f^4 \Phi(f)_{\Delta n}\, df}{\int_0^\infty f^2 \Phi(f)_{\Delta n}\, df} \quad \text{(ref. 4)}$$

m total number of observations

N total number of positive peaks exceeding a given value

n normal load factor, g units

$n(t)$ time history of normal load factor

n_L service limit normal load factor

Δn incremental normal load factor $(n - 1)$

Δn_L incremental service limit normal load factor $\left(n_L - 1\right)$

$\overline{\Delta n}$ mean incremental normal load factor

$\Delta n''$ filtered value of incremental normal load factor; at time t, $\Delta n_t'' = 0.9\Delta n_{t-\Delta t} - 2\Delta n_t + 0.9\Delta n_{t+\Delta t}$

Δn_0 value of Δn at point of truncation

$P(y)$ probability that a given value y will be exceeded

$P_N(y)$ probability that a given value y will be exceeded based on a normal probability distribution

P_1 probability of exceeding a given load-factor peak for load factors greater than 1

T total flight time

T_M maneuvering flight time

t time, sec

Δt time reading interval, sec

$\alpha(\zeta)$ proportion of area of normal curve represented by data in a truncated distribution

$\delta(f-0)$ Dirac delta function at $f = 0$

ξ mean of parent distribution from which truncated distribution is derived

σ root-mean-square value of Δn, $\sigma^2 = \frac{\Sigma(\Delta n - \overline{\Delta n})^2}{m} = \int_0^\infty \Phi(f)_{\Delta n}\, df$

$\Phi(f)_{\Delta n}$ power spectral density of incremental normal load factor (Δn),

$$g^2/\text{cps}, \quad \Phi(f)_{\Delta n} = \lim_{T \to \infty} \frac{1}{T} \left| \int_{-T}^{T} n(t) e^{-2\pi i f t} dt \right|^2 \quad \text{(ref. 2)}$$

$\Phi(f)_{\Delta n''}$ power spectral density of $\Delta n''$

χ^2 statistical reliability parameter

$\chi^2_{.05}$ critical statistical reliability parameter

AIRPLANES

The airplanes for which data were obtained were service models of the Republic F-84G and the North American F-86A. Both are low-wing

jet-propelled fighter-type airplanes, the F-86A having a swept wing and empennage. The F-86A was equipped with an adjustable stabilizer and a hydraulically boosted elevator.

The power spectra presented herein were obtained from flights made with external fuel tanks for the F-84G and without external fuel tanks for the F-86A. Except for the addition of sideslip and angle-of-attack booms, neither the external appearance nor the weight and balance of the airplanes was altered by the addition of the NACA instrumentation. Three-view drawings of the airplanes are presented in figure 1.

INSTRUMENTATION AND TESTS

The data were measured by standard NACA photographically recording instruments. In order to relieve the pilot of any recording-instrument switching procedure and thus to assist in obtaining normal operation, a pressure switch was employed to operate the recording instruments automatically at take-off.

Normal load factors (normal to the longitudinal reference) were measured by an NACA air-damped recording accelerometer. The measuring element was damped to about 0.65 of critical damping and the natural frequency was about 20 cycles per second. The accelerometer was located near the airplane center of gravity in such a way that the effects of angular velocities and angular accelerations were negligible.

A standard two-cell pressure recorder connected to the airplane service system was used to measure the pressure altitude and indicated airspeed. The service systems were of the usual total-pressure-tube and flush static-pressure-orifice type. No corrections were made to the measurements for position error associated with the location of the static orifices.

The flights were performed by service pilots during regular squadron operational training. Data were recorded continuously throughout a flight and were recorded only during those flights in which the mission was scheduled to include a large number of maneuvers. Although not requested, most of the maneuvers were performed in relatively smooth air. No attempt was made to specify the type or severity of maneuvers. Although the pilots were aware of the instrumentation, it was stressed that this was not to restrict their normal handling of the airplane since they would not be personally identified with the test results.

The flights for which power spectra were obtained were selected since they contained most of the tactical maneuvers that are within the capabilities of the individual airplanes. A summary of the operations and

flight conditions for these flights is presented in the following table and includes the actual amounts of time from which the spectra were obtained. Distributions of the percentage of time (used for spectra) spent in various altitude and airspeed ranges for two combined flights of the F-84G and three combined flights of the F-86A are shown in figures 2 and 3, respectively.

Airplane	Flight	Pilot	Mission	Average weight, lb	Average pressure altitude, ft	Average indicated airspeed, knots	Average Mach number	Time for which spectrum was obtained, sec
Republic F-84G	1	A	Acrobatics and dive-bombing	16,000	11,000	290	0.53	3,900
	2	B	Acrobatics, dive-bombing, and ground gunnery					2,777
North American F-86A	1	C	Acrobatics	13,060	14,150	298	.58	1,876
	2	C	Acrobatics					1,823
	3	D	Dogfighting					1,032

METHODS OF ANALYSIS

Power Spectral Densities

In the present paper use will be made of some of the concepts from the theories and methods of power spectral analysis. The methods used in the present paper are described in references 2 and 3.

The methods described in reference 2 were used in determining the power-spectral densities of the normal-load-factor data. The records were read at 0.5-second intervals for each flight and 40 estimates of the power at frequencies up to 1 cycle per second were obtained by using digital computing methods. In order to improve the accuracy of the computed spectra, the spectra were first obtained of an altered (filtered) time history of load factor given by the equation

$$\Delta n_t'' = 0.9\,\Delta n_{t-\Delta t} - 2\,\Delta n_t + 0.9\,\Delta n_{t+\Delta t} \qquad (1)$$

This is essentially a high-pass filter which retains some information at zero frequency. This particular expression was used since it was found to make the spectrum of $\Delta n''$ relatively constant over the frequency range. The spectrum of $\Delta n''$ was then converted to the spectrum of Δn by the equation

$$\Phi(f)_{\Delta n} = \frac{\Phi(f)_{\Delta n''}}{(1.8 \cos 2\pi f \Delta t - 2)^2} \tag{2}$$

In addition to the spectra computed from the records read at 0.5-second intervals, spectra were also computed from the data taken at 2-second intervals and at 10-second intervals in order to provide more detail on estimates of power at the lower frequencies. The spectra computed for 2-second intervals were computed for each flight at frequencies up to 1/4 cycle per second. The spectra computed for 10-second intervals were computed for the combined individual flights for each airplane at frequencies up to 1/20 cycle per second. The data at 10-second intervals were not filtered by using equation (1) since the spectrum was relatively level.

Ordinarily spectra are obtained of quantities which fluctuate about some mean value. Maneuver load time histories, on the other hand, fluctuate about 1 g but generally only in the positive direction.

The power spectral densities of the incremental maneuvering load with a nonzero mean $(\overline{\Delta n})$ would include a Dirac delta function at the origin with an area $(\overline{\Delta n})^2$:

$$\Phi(f)_{\Delta n_1} = 2\overline{\Delta n}^2 \delta(f-0) + \Phi(f)_{\Delta n} \tag{3}$$

The power spectra presented in this paper have the mean taken out and are equal to the last term $\Phi(f)_{\Delta n}$ in equation (3).

Load-Factor Counts

Threshold counts.- The probability curves for the normal-load-factor data were determined by a process which minimized the level-flight portions of the record. In this method counts were made at a given threshold every time the record crossed the given threshold and exceeded one-half of the increment to the next threshold. In this paper threshold values of 0.5g were used. For example, counts were made at 2g if the load-factor record crossed 2g while increasing and then increased beyond 2.25g or if the record crossed 2g while decreasing and decreased beyond 1.75g. This method is illustrated in figure 4

(method 3). In using this method all small fluctuations in the load factor less than $\pm 0.25g$ are eliminated.

Peak counts.- Two methods of obtaining major peak distributions were used in this paper and are illustrated in figure 4. In the first method (method 1) peaks were counted with a threshold of $0.25\Delta n$ or $0.25g$ whichever was greater; that is, the load factor must decrease more than one-quarter of the value of the peak-load-factor increment Δn before and after the peak. For values of Δn below 1 (2g), however, a threshold of $0.25g$ was used in which the load factor had to decrease $0.25g$ before and after the peak. The second method (method 2) was method B of reference 1. In both methods peaks of less than $0.25g$ were not counted. Peaks obtained by using method 2 were counted manually. Those obtained by using method 1 were counted automatically from the time histories with a digital computer.

RESULTS AND DISCUSSION

Spectrum for F-84G Airplane

In figure 5 the power spectrum of normal load factor is shown for flight 1 for the F-84G airplane. Results are shown for the four quarters of the flight, of which each part consisted of about 900 seconds of flight. The root-mean-square value σ and the mean $\overline{\Delta n}$ for each part are shown in the figure.

The power spectral densities for each of the four parts appear to be very similar and decrease approximately with f^{-3}.

The total spectrum for flight 1 of the F-84G airplane is shown in figure 6. Also included is the spectrum of the data taken at 2-second intervals to provide more detail at the lower frequencies. In addition, the statistical 95-percent confidence bands associated with the spectrum are shown. For simplicity, the confidence bands shown were obtained for a faired curve rather than for each individual point. The value of $\Phi(f)_{\Delta n}$ at zero frequency shown has little statistical reliability and is shown only as a matter of interest.

The confidence bands shown in figure 6 are representative of those obtained for all the spectra presented in this paper. Therefore, confidence bands for the other spectra will not be given.

The spectrum obtained with $\Delta t = 2$ seconds provides more detail at the lowest frequencies and generally agrees with the spectrum obtained with $\Delta t = 1/2$ second except at the highest frequencies. At the highest

frequencies for the 2-second data (i.e., 1/4 cps) the spectrum is not expected to be accurate since the power at higher frequencies is included in the spectrum obtained. Therefore the values for the 2-second data are not shown at the higher frequencies.

Effect of level flight on spectrum.- The effect of the presence in the time history of long intervals at 1 g or level flight on the spectrum is shown in figure 7. The results shown are for about 900 seconds from flight 2. The record was examined and approximately 530 seconds of flight near 1 g were deleted. The resulting record was then analyzed with one maneuver connected to the end of the previous one. The results are presented as the power spectral densities divided by the mean square σ^2 of the respective parts. The value of σ^2 of the original time history was 0.398 and the value of σ^2 for the all-maneuvering time history (original less level flight) was 0.929. It may be seen from figure 7 that above 0.025 cycle per second the spectra are directly proportional to the mean square or

$$\left[\frac{\Phi(f)_{\Delta n}}{\sigma^2}\right]_T = \left[\frac{\Phi(f)_{\Delta n}}{\sigma^2}\right]_{T_M} \tag{4}$$

where T_M refers to the maneuvering flight time and T to the total flight time. In addition,

$$\frac{\sigma^2_T}{\sigma^2_{T_M}} \approx \frac{T_M}{T} \approx \frac{\left[\Phi(f)_{\Delta n}\right]_T}{\left[\Phi(f)_{\Delta n}\right]_{T_M}} \tag{5}$$

In general, the effect of level flight on the spectrum is to change the level of the spectrum.

Spectra for flights 1 and 2.- In figure 8 the spectra for the complete flights 1 and 2 are given. In each case the power has been divided by the mean square for the particular flight. The power spectral densities are seen to be quite similar for the two flights. At the higher frequencies (above 0.1 cps) the two curves have the same shape but are of different magnitudes.

In figure 9, flights 1 and 2 have been combined and, in addition, the power spectral densities obtained for the combined flights 1 and 2 at 10-second intervals have been included. The 10-second data have been corrected for "folding" based on the spectra obtained from the 1/2-second and 2-second data. When the 10-second data are included, a peak appears at about 0.025 cycle per second which corresponds to the average number of maneuvers per second during the two flights, which is roughly 0.024 (86 maneuvers per hour).

Spectra for F-86A Airplane

The power spectral densities for three operational flights of the F-86A airplane are shown in figure 10. The results are ratioed to the mean square values of the incremental load factor. The spectra for these three operational flights also appear to be similar.

The power spectral densities for the combined flights 1, 2, and 3 for the F-86 airplane are shown in figure 11. Included in this figure are the data obtained at 10-second intervals. As was the case for the F-84G airplane, there appears to be an indication of a peak in the spectrum at approximately 0.02 cycle per second. Again this value corresponds to the average number of maneuvers per second in flights 1, 2, and 3 of about 0.022 (79 maneuvers per hour).

Comparison of Spectra for F-84G and F-86A Airplanes

In figure 12 are shown the normalized power spectral densities for three combined flights for the F-86A airplane and two combined flights of the F-84G airplane. The same curves are shown on a linear scale in figure 13.

The power spectral densities for the two airplanes in squadron operations are very much alike (fig. 12); however, there appears to be some increase in power at the highest frequencies (1 cps) for the F-86 airplane as compared with the F-84G airplane. It is believed that this increase is caused by a lightly damped longitudinal oscillation which was present in the F-86 airplane. The effect of this is probably present at frequencies between 0.4 and 1 cycle per second. In figure 12 the power spectral densities are shown to be relatively constant at frequencies below 0.03 cycle per second. The power is very low above 0.2 cycle per second. (See fig. 13.)

Analytical Representation of Maneuver Load Spectrum

The spectra of figure 12 appear to be of the type given by the formula for the simple spectrum:

$$\Phi(f)_{\Delta n} = \frac{\Phi(0)_{\Delta n}}{1 + \left(f/f_B\right)^a} \tag{6}$$

where f_B is the "break" frequency. In figure 14 the total spectra for the F-84G and F-86A airplanes (shown in fig. 12) were averaged according to the flight time for each airplane and are compared with equation (6). In this case a was found to be 2.6 and f_B was 0.031 cycle per second.

This equation appears to fit the data above a frequency of 0.005 cycle per second. Also shown in the figure as a matter of interest is the approximate phugoid frequency range which is between 0.008 and 0.025 cycle per second. As previously noted, the average number of maneuvers per second was 0.022 and 0.024 per second for these airplanes (79-86 per hour).

Probability Distributions

Threshold distributions.- The frequency distribution of threshold counts of normal load factor for the combined three flights of the F-86A airplane is shown in figure 15 and table I. In examining the frequency distributions, it was noted that the distributions looked much like normal distributions if only the positive or only the negative distributions were examined. For example, in figure 15, normal-distribution curves are shown for both the positive and the negative distributions. These curves may be described as truncated normal distributions above and below $\Delta n = 0$. (See ref. 6 for a discussion of truncated distributions.) Since the distributions are essentially one sided, the measured value of the threshold counts at $\Delta n = 0$ must be adjusted. Therefore, in figure 15 it may be noted that the zero value for the positive side is given as two times the number of zero threshold values having a positive slope, and, in a similar manner, the zero value for the negative side is given as two times the number of zero threshold values having a negative slope. In table I the threshold counts labeled 0 are the zero values having positive slope and those labeled (-)0 are the zero values having negative slope.

The probability of exceeding a given incremental normal load factor Δn_{tr} for a truncated normal distribution is

$$P\left(\Delta n_{tr}\right) = \frac{1}{\alpha(\zeta)\sqrt{2\pi}} \int_{\frac{\Delta n_{tr}-\xi}{\sigma}}^{\infty} e^{-\frac{1}{2}Z^2}\, dZ \qquad (7)$$

for $\Delta n_{tr} \geqq 0$

where

$$\Delta n_{tr} = \Delta n - \Delta n_0$$

and

$$Z = \frac{\Delta n_{tr} - \xi}{\sigma}$$

The normal-load-factor data are truncated at $\Delta n = 0$ and the mean of the parent distribution is assumed to be at $\Delta n = 0$. Therefore,

$$\alpha(\zeta) = 0.50$$

$$\xi = 0$$

and

$$P(\Delta n) = \frac{1}{0.5\sqrt{2\pi}} \int_{\Delta n/\sigma}^{\infty} e^{-\frac{1}{2}\left(\frac{\Delta n}{\sigma}\right)^2} d\left(\frac{n}{\sigma}\right) \qquad \Delta n \geq 0 \qquad (8)$$

L 1 5 5 7

Since it is sometimes convenient to examine data on normal probability graph paper, the quantity $\alpha(\zeta)P(\Delta n)$ of a truncated normal distribution can be plotted and the results will fall in a straight line on normal probability paper.

The probability distributions of threshold counts of normal load factor for flights 1 and 2 of the F-84G airplane and flights 1, 2, and 3 of the F-86A airplane are shown on a normal probability scale in figures 16 and 17. The data are shown for the individual flights as well as for the combined flights for each airplane. The value $\alpha(\zeta)P(\Delta n)$ is plotted against Δn. In each case, the zero value used was two times the number of zero thresholds having a positive slope. The threshold counts for each airplane are given in table I. The points shown in figures 16 and 17 are plotted at 1/4g less than the threshold values used (i.e., 1 plotted at 0.75, 1.5 plotted at 1.25, and so forth) since the thresholds were based on bands ±1/4g about the threshold values.

In figures 16 and 17 it may be seen that the truncated normal distributions appear to fit the data. In addition to the plots on the normal probability scale the χ^2(Chi-square) statistical test was made for each flight and the combined flights. (See ref. 7, for example.) The results of these tests as shown in the figures are well within the 95-percent level of significance and indicate that the maneuvering loads of the operational flights presented in this paper can be considered as truncated normal distributions.

Although similar analysis could be made of the negative maneuvering load factors, the data sample sizes used were not sufficient for any reliable analysis to be made.

Peak-load distribution.- The peak-load-factor frequency distributions obtained for the combined flights of each of the airplanes are given in table I. Two peak distributions are given: the total peak distribution and the major peak distribution. The total peak distribution includes all peaks obtainable from the time histories of normal

load factor. Since the load factors were calculated to 0.001g, the threshold for the total distribution is 0.001g, which is less than the reading accuracy of about 0.01g. A count was made of all the peaks by using a threshold value of 0.01g for the F-84G airplane and it was found that the difference between the frequencies counted by using the two thresholds was almost entirely included in the 0 to 0.25g range. Therefore, the values beyond 0.25g are probably not affected to any extent by the threshold used. In addition, since the records were read at 0.5-second intervals the minor peaks at high frequencies were also filtered out; however, these are not believed to be of any importance in these flights.

In figures 18 and 19 the major peak cumulative frequency distributions are shown plotted against $(\Delta n)^2$ for the F-84G and F-86A airplanes. Also plotted in figures 18 and 19 are the threshold frequency distributions. From equation (8) it may be seen that the threshold frequencies should plot as a straight line when plotted against $(\Delta n)^2$ on semilog paper if the distribution is a truncated normal distribution. Also it may be seen from figures 18 and 19 that the major peak cumulative distribution plots approximately as a straight line against $(\Delta n)^2$ above $\Delta n = 1$.

Calculated peak-load distributions.- In reference 4 an expression for the probability of exceeding a given peak is given for a Gaussian random process. Although the maneuvering load data of this paper cannot be considered a Gaussian random process, the results of figures 16 and 17 indicate that the positive maneuver loads can be considered as a truncated or "half" normal distribution. Therefore, it was believed that perhaps the peak probability expression given in reference 4 might be used as a guide in calculating the peak distributions obtained in the present tests.

If the maneuvering loads were Gaussian in character the probability that a peak load will exceed a given value can be given, as in reference 4, as

$$P(\Delta n) = P_N\left(\frac{\Delta n/\sigma}{K_1}\right) + \frac{f_0}{f_p} e^{-\frac{1}{2}\left(\frac{\Delta n}{\sigma}\right)^2}\left[1 - P_N\left(\frac{\Delta n/\sigma}{K_2}\right)\right] \tag{9}$$

where

$$K_1 = \sqrt{1 - \left(f_0/f_p\right)^2}$$

and

$$K_2 = \frac{K_1}{f_0/f_p}$$

and where the normal probability distribution $P_N(y)$ is

$$P_N\left(\frac{\Delta n}{K_i\sigma}\right) = \frac{1}{\sqrt{2\pi}}\int_{\frac{\Delta n}{K_i\sigma}}^{\infty} e^{-\frac{1}{2}\left(\frac{\Delta n}{K_i\sigma}\right)^2} d\left(\frac{n}{K_i\sigma}\right) \tag{10}$$

where $i = 1$ or 2.

The total number of positive peaks exceeding a given value is

$$N = f_p T_M P(\Delta n) \tag{11}$$

For large values of Δn equation (9) approaches

$$P(\Delta n) \approx \frac{f_0}{f_p} e^{-\frac{1}{2}\left(\frac{\Delta n}{\sigma}\right)^2} \tag{12}$$

and for the asymptotic case the number of peak loads exceeding a given value approaches

$$N \approx f_0 T_M e^{-\frac{1}{2}\left(\frac{\Delta n}{\sigma}\right)^2} \tag{13}$$

Since much of the flight time is spent in nonmaneuvering or near-level flight, the maneuvering flight time rather than the total flight time is used in equations (11) and (13). In order to determine the maneuvering flight time, the percentage of total flight time spent above a given load factor was determined. These times are shown in figure 20 for the F-84G airplane and in figure 21 for the F-86A airplane. The distribution of the time spent in various load-factor intervals is given in table II. Since in the threshold counts and in the peak counts the minimum load-factor variation was 0.25g, it was assumed that the maneuvering flight time was the portion spent above $\Delta n = 0.25g$. It can be seen in figures 20 and 21 that about 52 percent of the total flight time could be considered maneuvering flight time for both the F-84G airplane and the F-86A airplane in these particular flights.

The peak-load data for the F-84G airplane are shown in figure 22 and the peak-load data for the F-86A airplane are shown in figure 23. Two peak-load distributions are shown - the total peak distribution and the major peak distribution. The major peaks shown in figures 22 and 23 were counted by both method 1 and method 2 of figure 4; however, only the results from method 1 are shown. The results from method 2 were almost the same as those from method 1.

The peak-load distributions as given by equations (11) and (13) are also shown in figures 22 and 23. The value of the root-mean-square load factor σ used was that obtained from the threshold analysis of figures 16 and 17. The value of f_0/f_p obtained from the integration of the spectrums was 0.184 for the F-84G airplane and 0.135 for the F-86A airplane. The value of f_0 was 0.076 for the F-84G airplane and 0.081 for the F-86A airplane.

It may be seen in figures 22 and 23 that both the total peak count and the major peak count are approximately estimated by equations (11) and (13), respectively. The agreement seems somewhat better for the F-86A airplane than for the F-84G airplane.

Although the total peak count is of interest, it is the major peak distribution which is of most value. For example, in fatigue analysis, it is believed that the major peak distribution would more accurately describe the life history of loads than would the total peak distributions.

Major peak-load distribution in service operations.- In order to compare the results from the spectrum analysis with more complete flight data from regular service operations the major load-factor peaks obtained in the service operations of references 1 and 8 to 11 are shown in figures 24 to 26. The airplanes for which information is presented in figures 24 to 26 are

Republic F-84E and G
North American F-86A, E, and F
North American T-28A
North American B-45A
North American AJ-1
Lockheed F-80A, B, and C
Lockheed F-94B
Lockheed TV-1
Lockheed P2V-3
Lockheed P2V-4
Grumman F8F-2
Grumman F9F-2B
McDonnell F2H-2
Douglas AD-4

All data in these figures were obtained during training operations unless otherwise stated. The data represent about 24,000 hours for fighter-type airplanes and about 2,000 hours for bomber-type airplanes. In order to prepare figure 24 the total number of load-factor peaks exceeding a given load factor N were plotted against the parameter $(\Delta n/\Delta n_L)^2$ for each airplane. A straight line was then fitted to the data above a value of $(\Delta n/\Delta n_L)^2$ of about 0.2, and the straight line extrapolated to the value $N = N_0'$ at zero-load-factor increment. The ratio N/N_0' of the number of load-factor peaks exceeding a given load factor to the extrapolated value of exceeding a value of $\Delta n/\Delta n_L = 0$, is plotted for each airplane in figure 24. The solid symbols in figure 24 represent less than 10 points and are considered less representative of the peak distributions than the other points. Also shown in figure 24 are the number of hours of flight represented by the data and the value of N_0'/T, the extrapolated value of the number of peaks to exceed 1 g per hour.

For large values of load factor the peak distribution is given in the form of equation (13):

$$N/N_0' = e^{-\frac{1}{2}\left(\frac{\Delta n/\Delta n_L}{\sigma}\right)^2} \tag{14}$$

where

$$N_0' = f_0 T \frac{T_M}{T} \tag{15}$$

and

$$N_0'/T = f_0 \frac{T_M}{T} \tag{16}$$

When plotted on semilog paper as in figure 24, equation (14) is a straight line with the slope $-\frac{1}{2\sigma^2}$. The values of the root mean square σ for the data shown vary between 0.25 and 0.33. The average value of σ in figure 24 is 0.284 and it appears that the straight line fits most of the data fairly well above $1\sigma\left((\Delta n/\Delta n_L)^2 = 0.0806\right)$ at least up to the limit load factor. Of course, the value of σ is to some extent a function of the mission of the airplane and it is possible that, for a specific mission, considerably different values than those shown in figure 24 could be obtained. For example, in figure 24, the training data for the F-84E and G airplanes were obtained in Korean operations in which the airplane was used mostly in air-to-ground missions. The value of the root mean square for these data appears to be considerably lower than that for the other airplanes. (This effect would also be apparent if the true service limit load factor was lower than that assumed (7.33) in figuse 24.) Most of the other training data shown in figure 24 for the other airplanes were obtained in training which included many types of missions.

It may be noted from equation (16) that, if it can be assumed that f_0 is about 0.08 and does not change, the percent of maneuvering flight time can be determined from the values of N_0'/T given in figure 24.

$$\frac{T_M}{T} = \frac{N_0'/T}{f_0} = \frac{N_0'/T}{(0.08)(3600)} \tag{17}$$

From the values of N_0'/T in figure 24 and from equation (17) it was determined that approximately 2 to 8 percent of the total flight time was spent in maneuvering in the Air Force training operations, about

2 to 6 percent was spent in maneuvering in combat operations in Korea, and between 7 and 24 percent in the NACA tests in operational training. The value of 52-percent maneuvering-flight time obtained for the five flights of figures 20 and 21 are applicable to just those particular flights which were more active than the average. This percentage is obviously a function of the airplane mission and would be higher for gunnery or dive bombing training than for other operations.

In addition to the data available from Air Force operations there are data obtained with V-G recorders from U. S. Navy operations. (See ref. 11.) These data are presented in figure 25 as plots of the time to exceed 1 g in maneuvers t_0' to the time to exceed a given load factor t. Since, in V-G records a true frequency count cannot be obtained at low load factors, the data were used only where the count appeared to be approaching the true frequency. The times to exceed a given load factor were plotted against $\left(\Delta n/\Delta n_L\right)^2$ and a straight line was fitted to the data and extrapolated to zero-load-factor increment and then the ratio of this extrapolated zero time t_0' to the time to exceed a given load factor was plotted in figure 25. It may be seen that

$$\frac{t_0'}{t} = \frac{N}{N_0'} \tag{18}$$

The straight line shown in figure 25 is that obtained from figure 24 with a value of $\sigma = 0.284$. The black symbols represent points which consist of less than 10 peaks. The line appears to fit the data fairly well for most of the airplanes shown.

In figure 26, data obtained from references 10 and 11 are shown for several large airplanes. Also shown is the line obtained from the data for the fighter-type airplanes of figures 24 and 25. It may be seen that the data for the AJ-1 and P2V-4 airplanes are close to the line; however, the data from the B-45 and P2V-3 airplanes appear to have a higher root-mean-square value than that of the line shown. It is evident that the line shown would probably not be a good estimation of the loads to be encountered in airplanes which are primarily nonmaneuvering airplanes such as large bombers, but would be of more use in more maneuverable airplanes. In addition, it is not believed that the results for other low-limit load-factor airplanes would necessarily indicate more severe use (as indicated for the B-45 and P2V-3 airplanes) than the line shown. It is believed that for any large bomber the type of mission would have a large effect on the slope of the line.

Other methods of treating load-factor peak distributions.- From the spectrum analysis it was indicated that the major peak-load distribution could be given by equation (13) above 1σ and this is also indicated

from figures 24 and 25. It can be seen that below 1σ, however, the peak-load distribution is not well represented by equation (13). One way of accounting for the peaks at low load factors is to assume that the major peak distribution is made up of two peak distributions having different values of σ. If such is the case, the probability of exceeding a load-factor peak greater than 1 g can be given as

$$P_1 = \frac{N}{f_0 T_M} = \frac{T_1}{T_M} e^{-\frac{1}{2}\left(\frac{\Delta n/\Delta n_L}{\sigma_1}\right)^2} + \frac{T_2}{T_M} e^{-\frac{1}{2}\left(\frac{\Delta n/\Delta n_L}{\sigma_2}\right)^2} \tag{19}$$

where

T_1 maneuvering time associated with σ_1

T_2 maneuvering time associated with σ_2

For the data of figure 24,

$$\sigma_1 = 0.284$$

$$\sigma_2 = 0.100$$

$$T_1/T = T_2/T = 0.50$$

In figure 27 the data of figure 24 are shown with the probabilities given by equation (19). The probability given by equation (19) is almost identical to the "Standard Probability Curve for Maneuvers" given in reference 1. It may be seen that the data are represented fairly well by equation (19).

In figures 22 and 23 it might be noted that, although the major peaks were approximated by equation (13), the curve from the equation which represented the total peak count appears to be similar in shape to the major peak count. Therefore the major peak count could be approximated by an equation similar to equation (9).

The number of load-factor peaks exceeding a given load factor divided by the number of load-factor peaks exceeding 1 g from equation (9) is

$$\frac{N}{N_0} = \frac{P}{P_0} = P_1 = \left(\frac{2}{1 + f_0/f_p}\right)\left\{P_N\left(\frac{\Delta n/\Delta n_L}{K_1\sigma}\right) + \frac{f_0}{f_p} e^{-\frac{1}{2}\left(\frac{\Delta n/\Delta n_L}{\sigma}\right)^2}\left[1 - P_N\left(\frac{\Delta n/\Delta n_L}{K_2\sigma}\right)\right]\right\} \tag{20}$$

When N/N_0 is plotted against $\left(\frac{\Delta n/\Delta n_L}{\sigma}\right)^2$ it is approximately linear above 2σ and has a zero intercept of about $\frac{1}{2}P_0$ (at least for the present case of $f_0/f_p = 0.160$). Therefore, if the total number of major peaks above a given load factor are plotted against $\left(\Delta n/\Delta n_L\right)^2$ and a straight line fitted to the data, the slope of the line will approximately determine the root-mean-square value σ. Taking into account that the straight-line extrapolation of equation (20) will have a zero intercept of $\frac{1}{2}P_0$ or $\frac{1}{2}N_0$ the experimental data such as those in figure 24 can be compared with equation (20) if it is plotted as $N/2N_0$. In this form $N/N_0 = P/P_0 = P_1$ which is the probability of exceeding a given load factor for load factors greater than 1 g. In figure 27 the data are compared with equation (20) in this manner and it is in fairly good agreement.

Thus, any of the three equations (13), (19), and (20) can be used to approximate the major peak-load probability curve. Probably equation (13) is the simplest if the shape of the curve below 1σ is unimportant. If the low load factors are important, for instance in some fatigue applications, equation (19) or (20) would be more desirable. In addition, probably none of these equations are valid much above the limit load factor since inadvertent maneuvers may affect the curves mostly at high load factors. (See refs. 1 and 12.)

CONCLUSIONS

The results of the power spectral analysis of the maneuvering load data indicate that spectral methods appear to have some promise in the statistical treatment of maneuver loads data. It is admittedly an almost empirical use of these methods; however, it is an attempt to describe more completely the complex process of maneuvering loads on airplanes other than by simple peak counts. In addition, it should be pointed out that the flights for which the spectra were obtained were training flights of a general nature in which several different missions were simulated and that the results for an airplane flying one specific mission could be much different. From the present analysis the following conclusions have been reached.

1. The maneuver-load-factor time histories of the five operational flights examined could be described by a truncated normal distribution.

2. The power spectral densities obtained were relatively constant at frequencies below 0.03 cycle per second and varied inversely with approximately the cube of the frequency at the higher frequencies up to 1 cycle per second. Above a frequency of 0.005 cycle per second the spectrum could be approximated by a simple spectrum equation.

3. The frequency content above 0.2 cycle per second (5-second period) was very low.

4. The load-factor peak distributions were estimated fairly well from the spectral analysis.

5. Peak-load data from about 24,000 hours of service operations of fighter-type airplanes appeared to agree reasonably well below the limit load factor with the type of equations obtained from spectrum analysis.

Langley Aeronautical Laboratory,
National Advisory Committee for Aeronautics,
Langley Field, Va., October 2, 1956.

L-1557

REFERENCES

1. Mayer, John P., Hamer, Harold A., and Huss, Carl R.: A Study of the Use of Controls and the Resulting Airplane Response During Service Training Operations of Four Jet Fighter Airplanes. NACA RM L53L28, 1954.

2. Press, Harry, and Tukey, J. W.: Power Spectral Methods of Analysis and Their Application to Problems in Airplane Dynamics. Vol. IV of AGARD Flight Test Manual, Pt. IVC, Enoch J. Durbin, ed., North Atlantic Treaty Organization (Paris), pp. IVC:1-IVC:41.

3. Press, Harry, and Houbolt, John C.: Some Applications of Generalized Harmonic Analysis to Gust Loads on Airplanes. Jour. Aero. Sci., vol. 22, no. 1, Jan. 1955, pp. 17-26, 60.

4. Huston, Wilber B., and Skopinski, T. H.: Probability and Frequency Characteristics of Some Flight Buffet Loads. NACA TN 3733, 1956.

5. Walls, James H., Houbolt, John C., and Press, Harry: Some Measurements and Power Spectra of Runway Roughness. NACA TN 3305, 1954.

6. Hald, A.: Statistical Theory With Engineering Applications. John Wiley & Sons, Inc., c.1952.

7. Hoel, Paul G.: Introduction to Mathematical Statistics. John Wiley & Sons, Inc., 1947.

8. Gray, Frank P.: Maneuver Load Data From Jet-Fighter Combat Operations. WADC-TN-55-12, Wright Air Dev. Center, U. S. Air Force, May 1955.

9. Gray, Frank P.: Flight Analyzer Data From Accelerated Service Tests of T-28A Aircraft. Memo. Rep. No. MCREXA83-4515-12-12, Air Materiel Command, U. S. Air Force, Feb. 23, 1951.

10. Gray, Frank P.: Maneuver Flight Load Data From Squadron Operation of B-45A Aircraft. WADC Tech. Note 56-13, Wright Air Dev. Center, U. S. Air Force, Feb. 1956.

11. Mayer, John P., and Harris, Agnes E.: Analysis of V-G Records From Ten Types of Navy Airplanes in Squadron Operations During the Period 1949 to 1953. NACA RM L54G23, 1955.

12. Mayer, John P., and Hamer, Harold A.: A Study of Means for Rationalizing Airplane Design Loads. NACA RM L55E13a, 1955.

TABLE I.- FREQUENCY DISTRIBUTION OF NORMAL LOAD FACTOR

Δn	Major peaks, method 1		Δn	Total peaks		Threshold counts				
	F-84G	F-86A		F-84G	F-86A	F-84G		F-86A		
	Flights 1 and 2	Flights 1, 2, and 3		Flights 1 and 2	Flights 1, 2, and 3	Flight 1	Flight 2	Flight 1	Flight 2	Flight 3
0	17	8	0	691	555	78	110	64	46	19
.2	41	22	.25	270	292					
.4	46	39	.50	163	182	164	225	118	96	50
.6	46	29	.75	98	95					
.8	35	17	1.00	74	115	158	164	92	81	41
1.0	33	24	1.25	57	70					
1.2	18	25	1.50	50	54	110	125	55	58	29
1.4	30	20	1.75	48	37					
1.6	24	12	2.00	35	43	64	106	37	43	23
1.8	16	11	2.25	33	28					
2.0	13	10	2.50	16	28	43	92	20	28	22
2.2	11	9	2.75	18	25					
2.4	11	6	3.00	18	13	28	63	7	13	17
2.6	8	8	3.25	14	13					
2.8	10	4	3.50	13	4	14	43	2	2	9
3.0	8	7	3.75	5	3					
3.2	8	10	4.00	8	3	2	28	1		5
3.4	6	2	4.25	2	1					
3.6	8	0	4.50	5	1		29			1
3.8	5	2	4.75	2						
4.0	4	2	5.00	0			14			
4.2	3	1	5.25	1						
4.4	2	0	5.50	2			8			
4.6	2	1	5.75	3						
4.8	1		6.00	1			2			
5.0	1									
5.2	0		(-)0			31	52	25	20	4
5.4	1		-.50			9	33	9	17	1
5.6	2		-1.00			1	1		3	
5.8	1									
6.0	1									

TABLE II.- FREQUENCY DISTRIBUTION OF TIME SPENT IN VARIOUS NORMAL-LOAD-FACTOR INTERVALS

n	Time, sec	
	F-84G	F-86A
	Flights 1 and 2	Flights 1, 2, and 3
-0.2 to -0.001	1	4.5
0 to .499	63.5	47
.5 to .599	51.5	29
.6 to .699	83	70.5
.7 to .799	124.5	127
.8 to .899	200.5	238.5
.9 to .999	477	456
1.0 to 1.099	1136.5	668
1.1 to 1.199	753.5	466
1.2 to 1.299	529	332
1.3 to 1.399	420.5	274.5
1.4 to 1.499	311	239
1.5 to 1.999	987.5	758.5
2.0 to 2.499	585	445.5
2.5 to 2.999	396	248
3.0 to 3.499	275	157.5
3.5 to 3.999	117	110
4.0 to 4.499	90.5	42
4.5 to 4.999	36.5	13
5.0 to 5.499	18	5.5
5.5 to 5.999	10	.5
6.0 to 6.499	4.5	
6.5 to 6.999	5	
7.0 to 7.499	1.5	

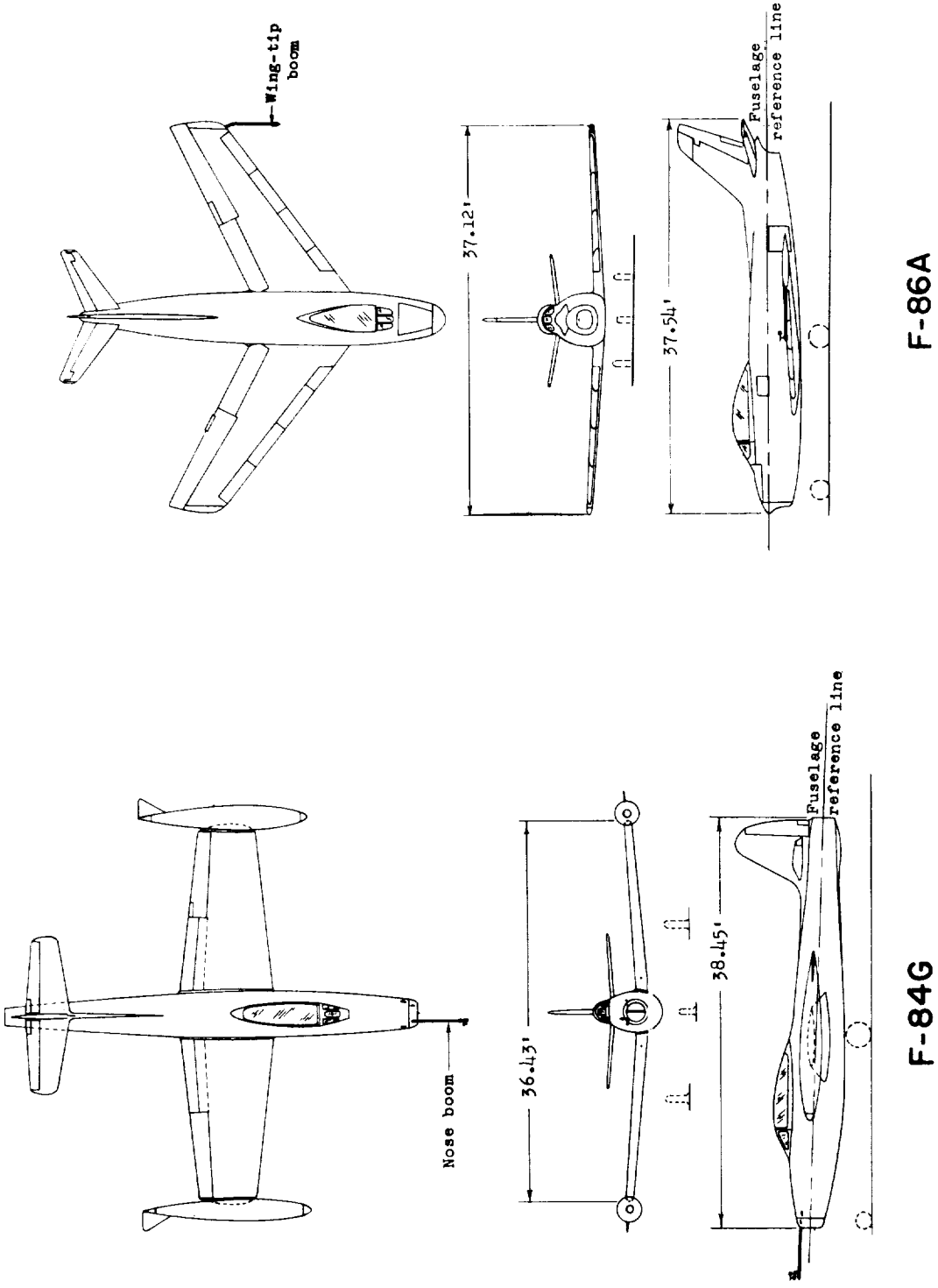

Figure 1.- Three-view drawings of test airplanes.

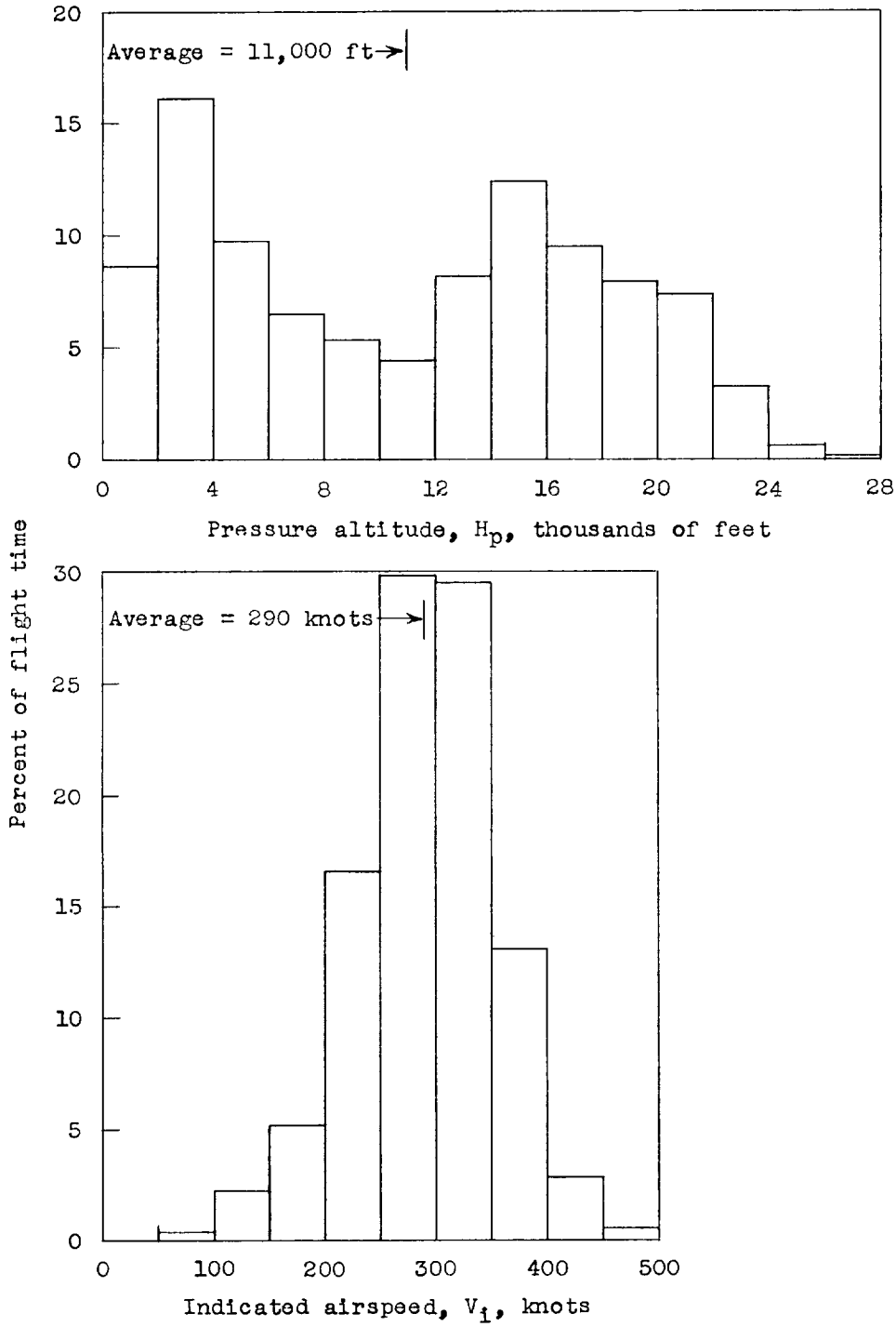

Figure 2.- Distribution of altitude and airspeed for flights 1 and 2 of the F-84G airplane.

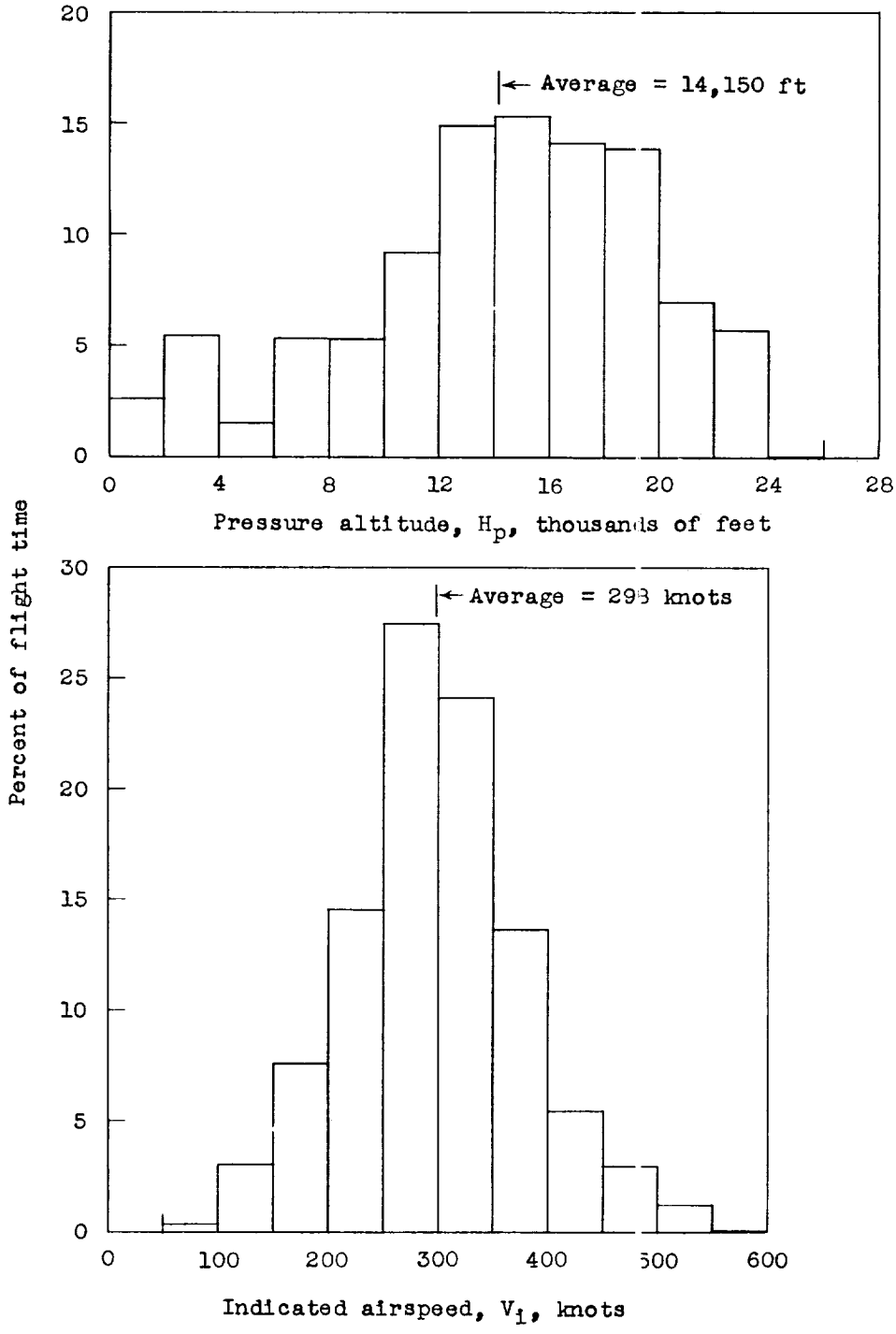

Figure 3.- Distribution of altitude and airspeed for flights 1, 2, and 3 of the F-86A airplane.

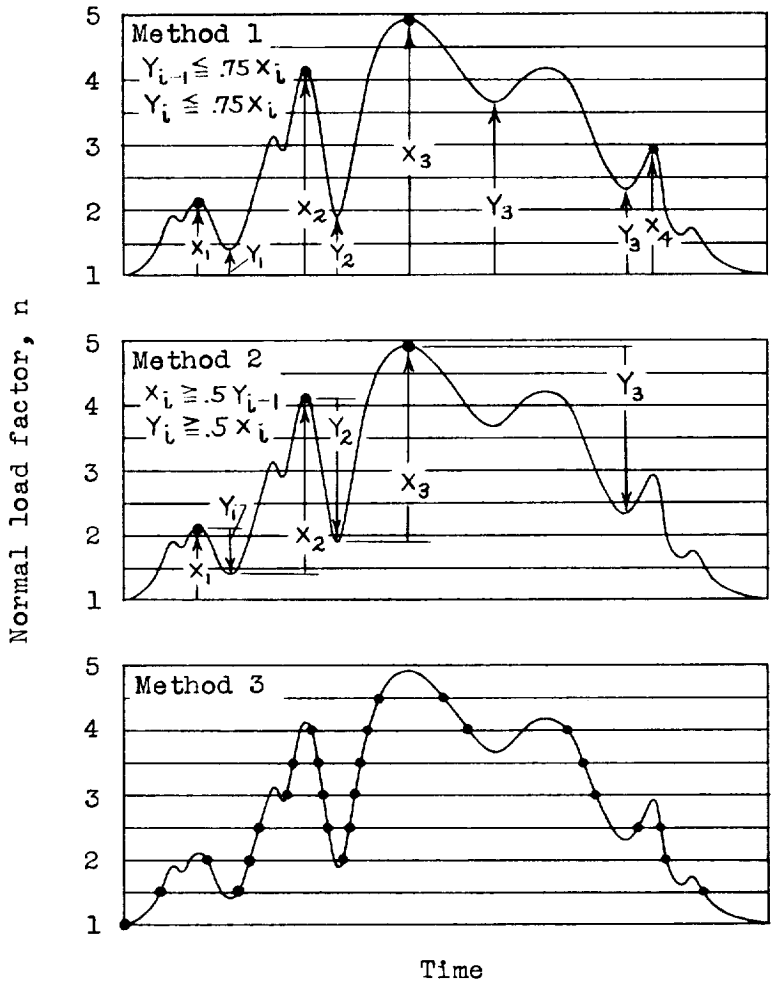

Normal load factor	Frequency count		
	Method 1	Method 2	Method 3
1.0			1
1.5			3
2.0	1	1	4
2.5	1		5
3.0			4
3.5			4
4.0	1	1	4
4.5	1	1	2

Figure 4.- Illustration of the three methods used for counting frequency distribution of normal load factor.

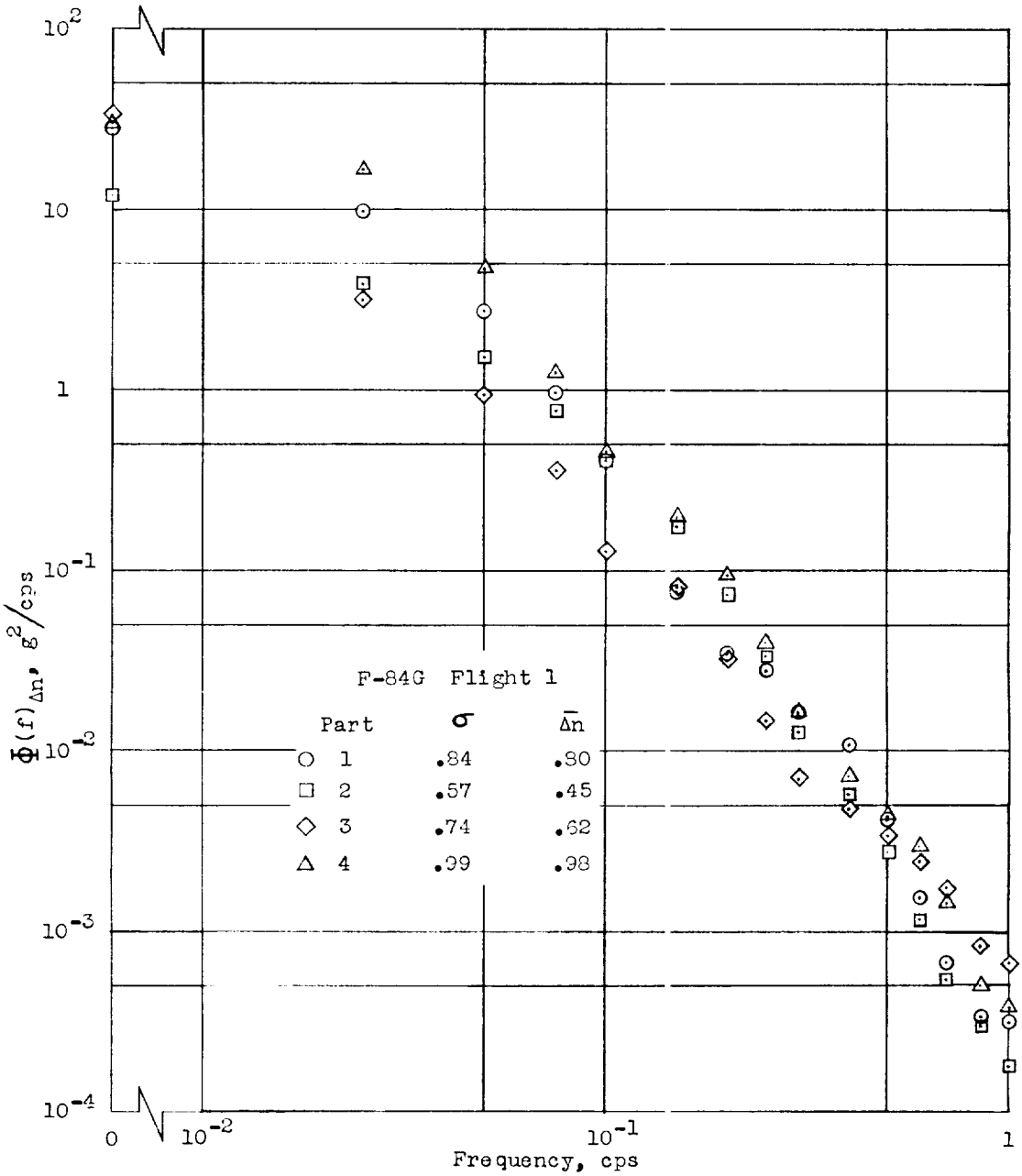

Figure 5.- Power spectral densities of normal load factor for four parts of flight 1, F-84G airplane.

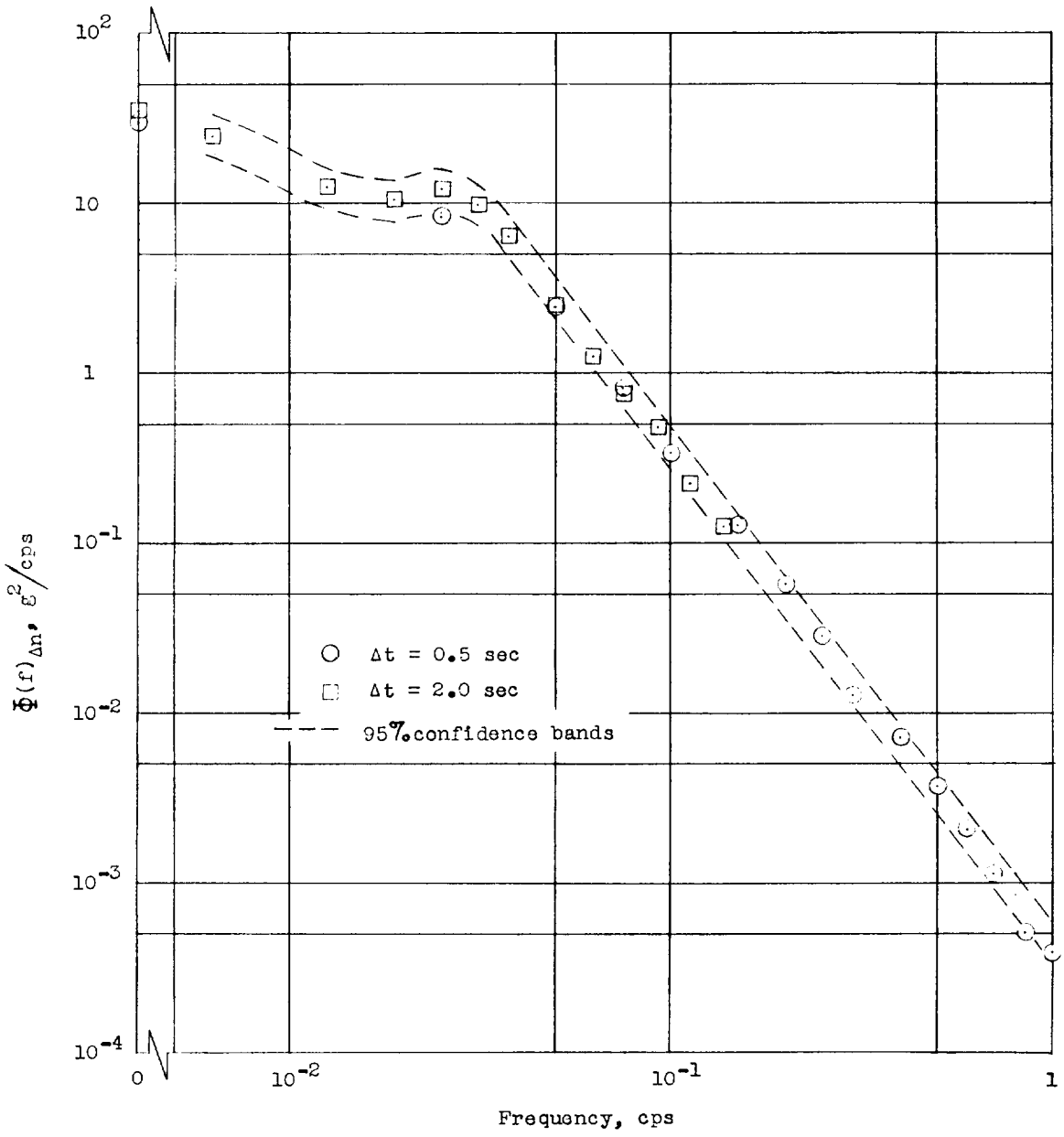

Figure 6.- Power spectral densities of normal load factor for flight 1, F-84G airplane.

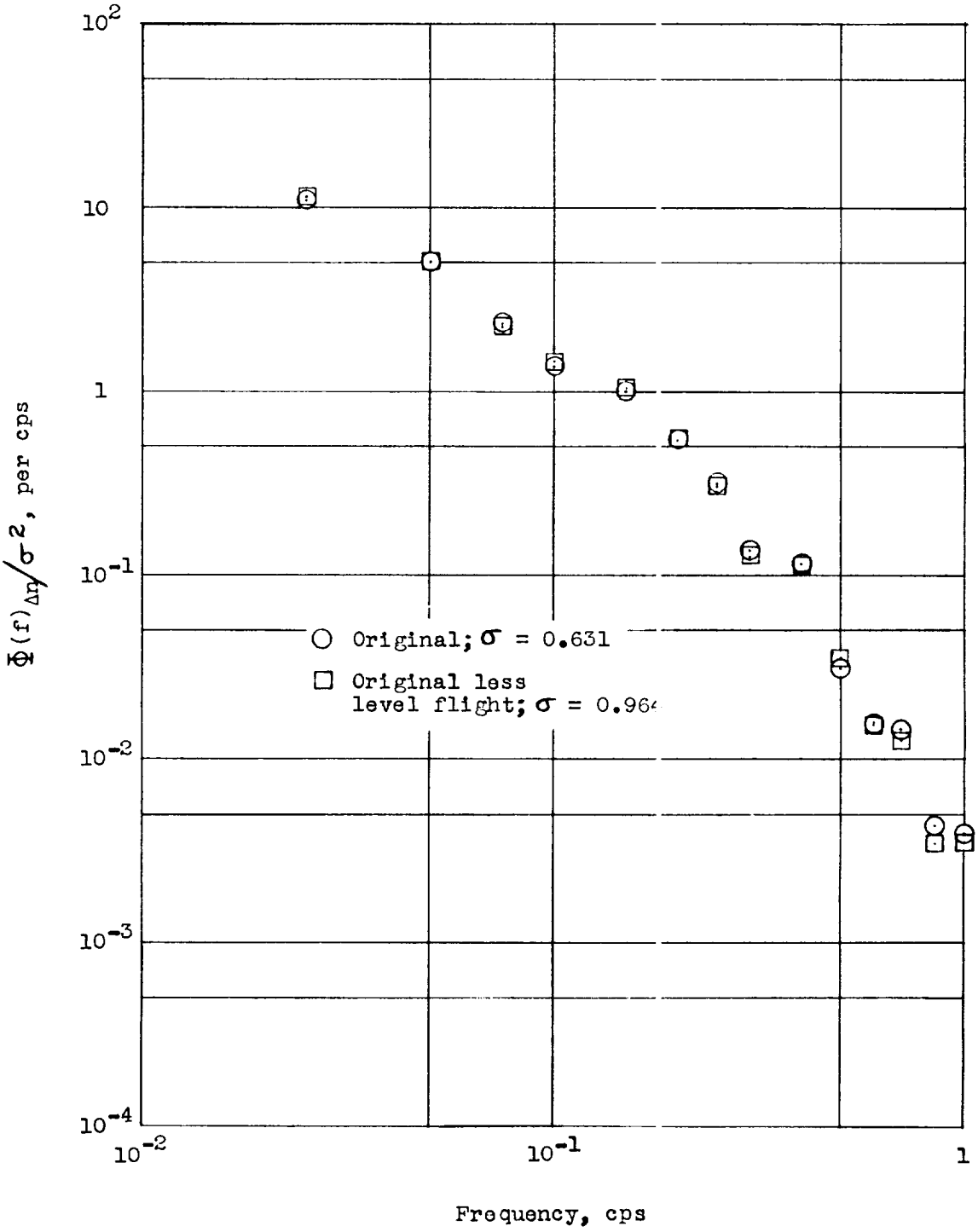

L-1557

Figure 7.- Effect of level flight on spectrum. F-84G airplane; 900 seconds of flight 2.

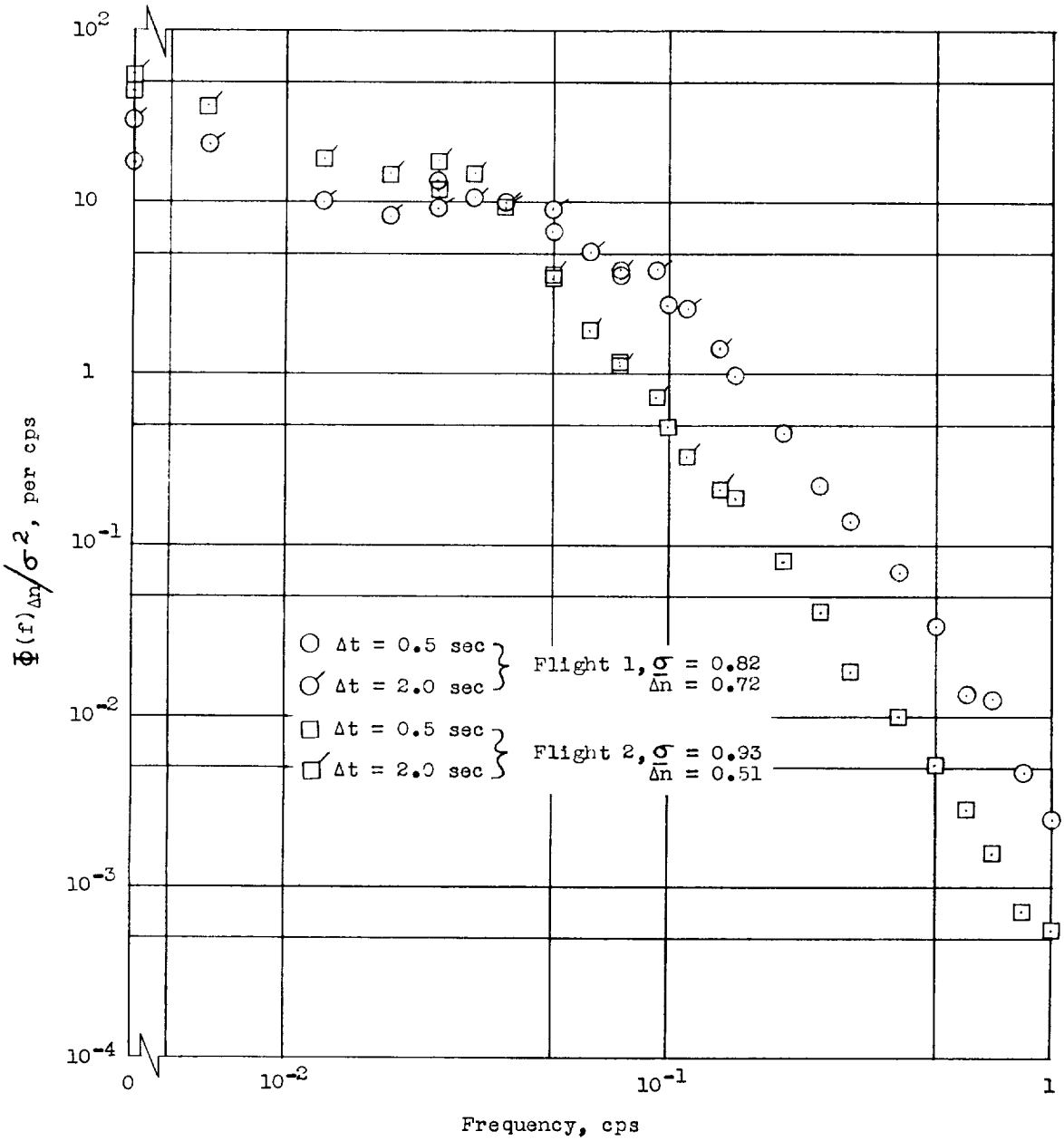

Figure 8.- Comparison of power spectral densities of normal load factor for two flights of the F-84G airplane.

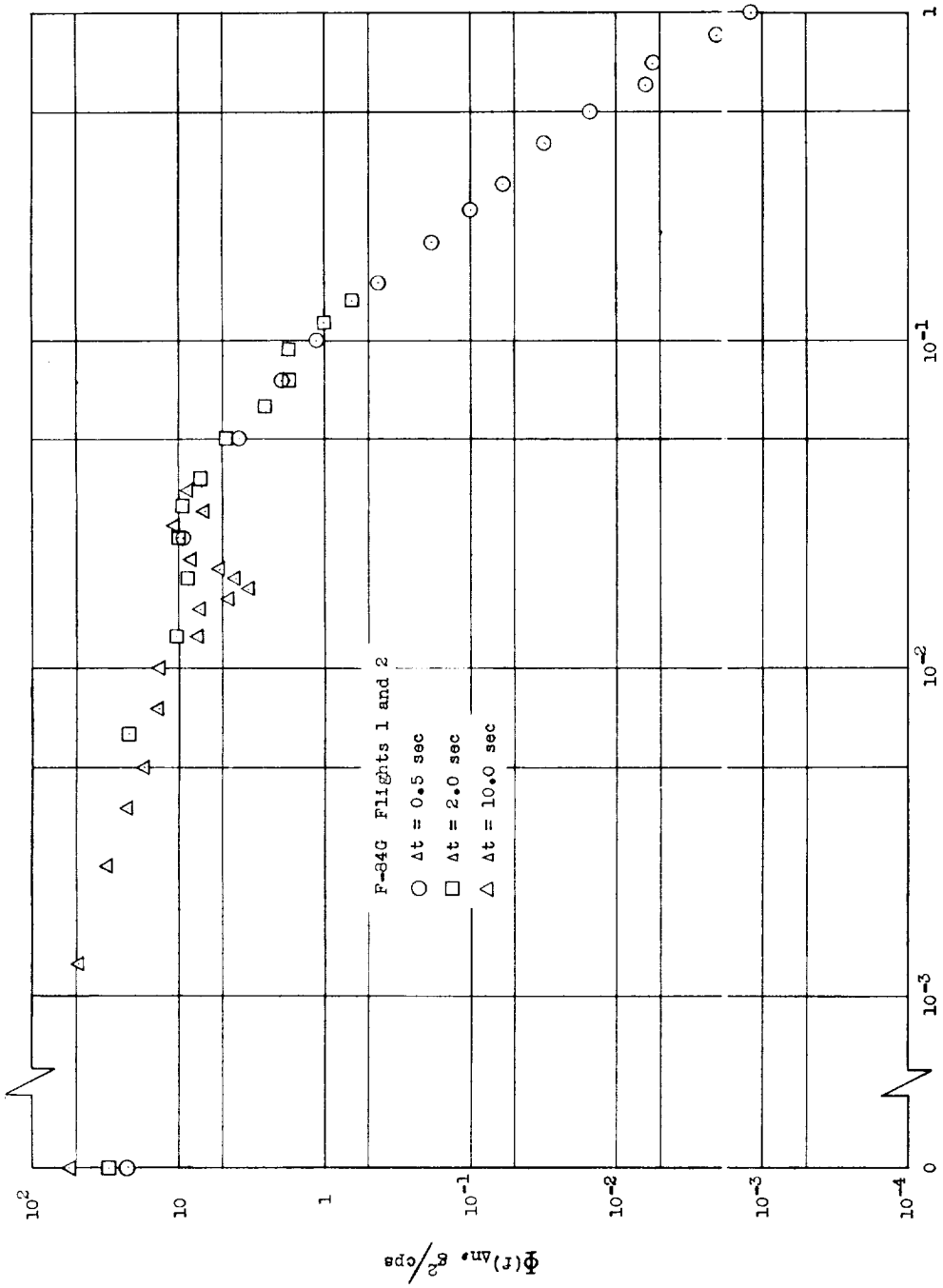

Figure 9.- Power spectral densities of normal load factor for two combined operational flights of the F-84G airplane.

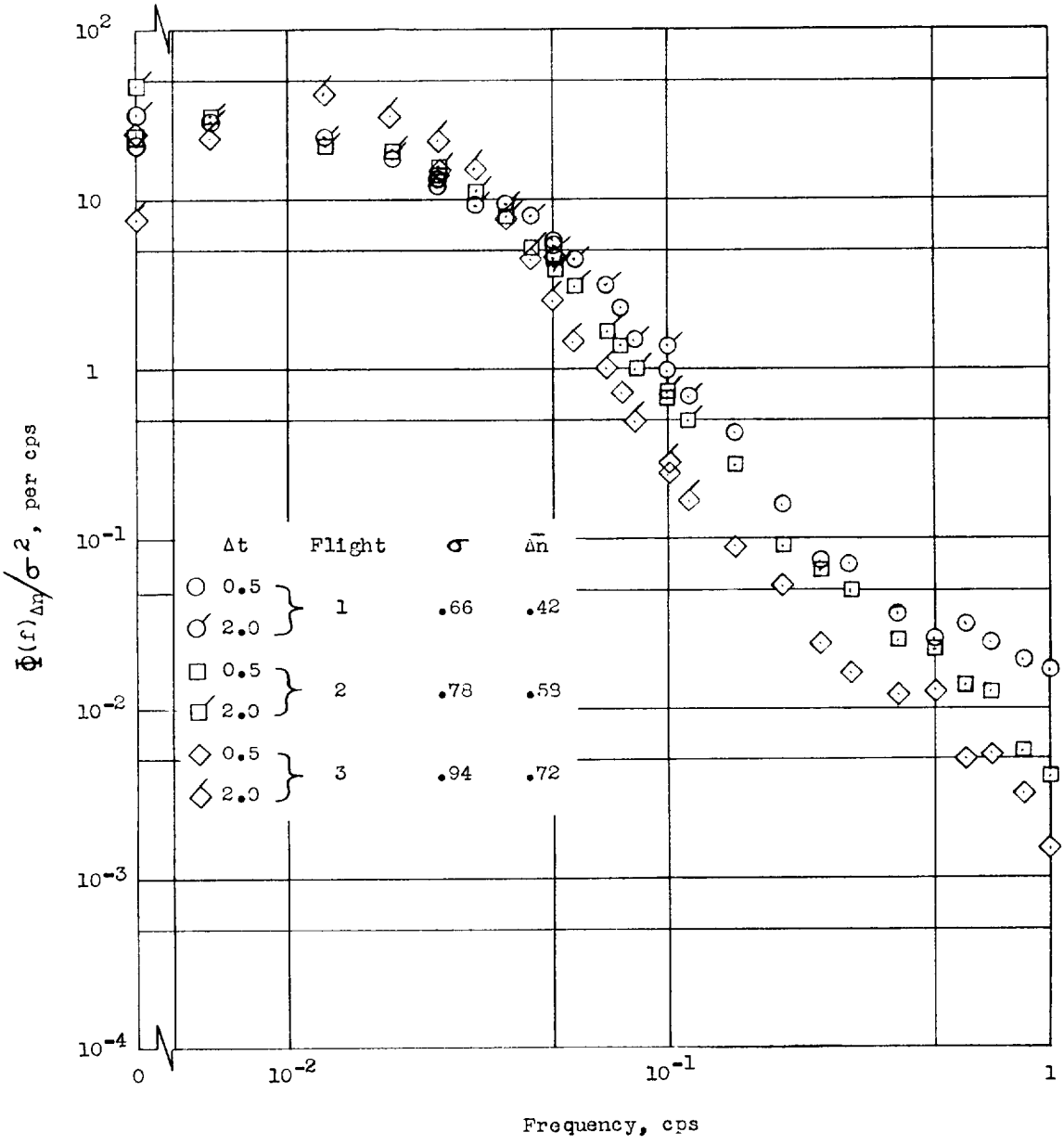

Figure 10.- Comparison of power spectral densities of normal load factor for three operational flights of the F-86A airplane.

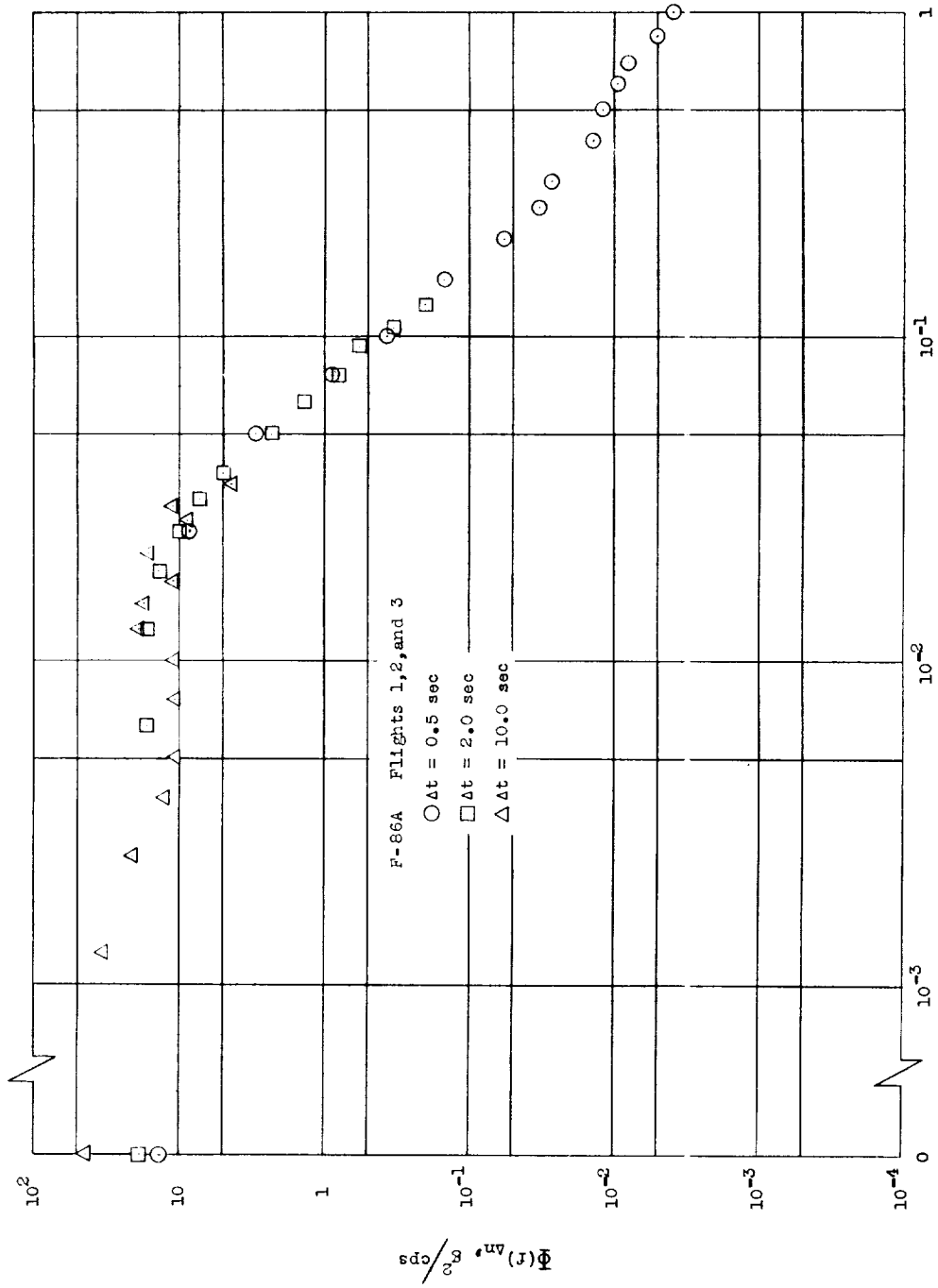

Figure 11.- Power spectral densities of normal load factor for three combined operational flights of the F-86A airplane.

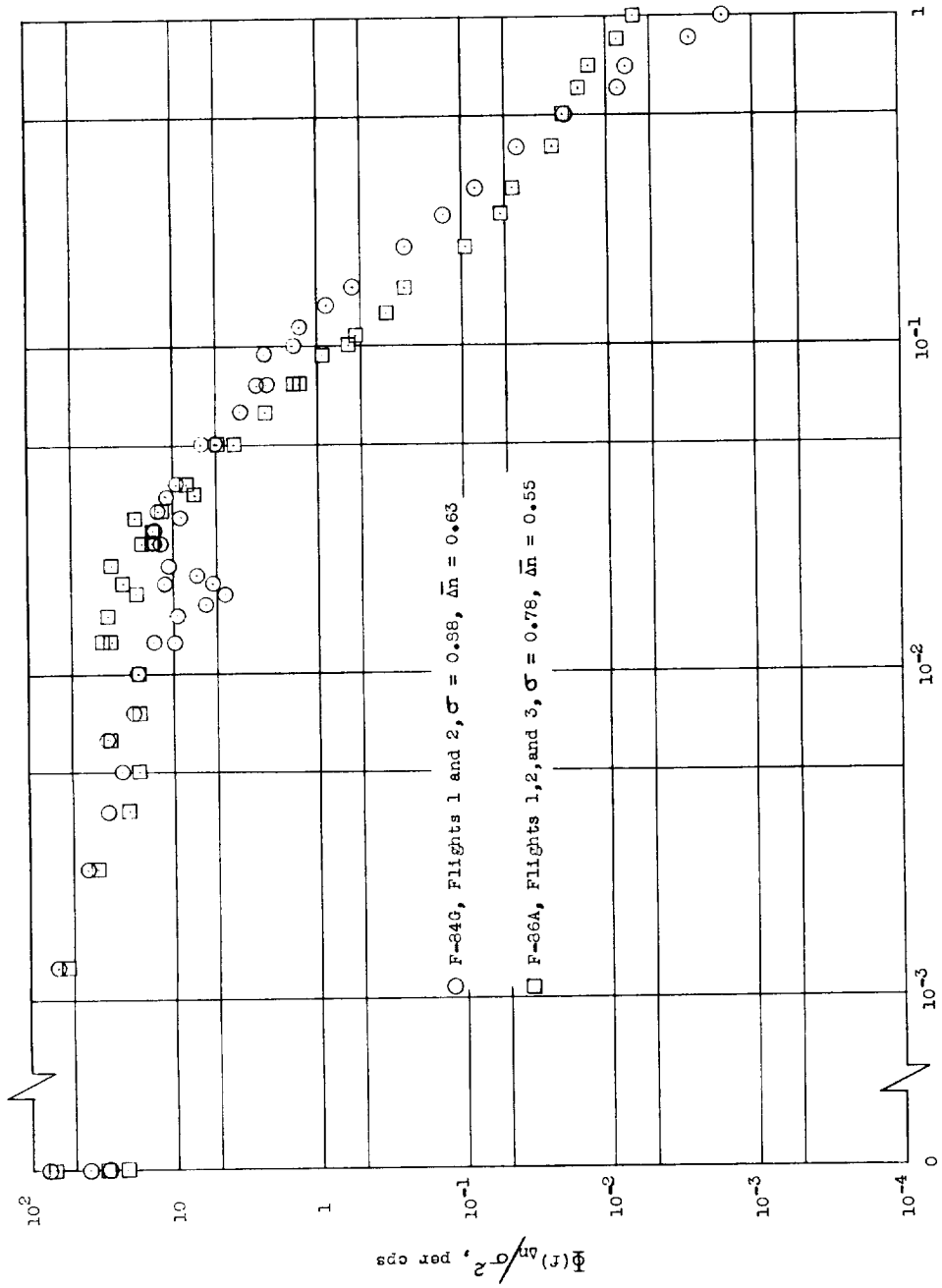

Figure 12.- Comparison of power spectral densities of normal load factor for two operational flights of the F-84G airplane with those for three operational flights of the F-86A airplane.

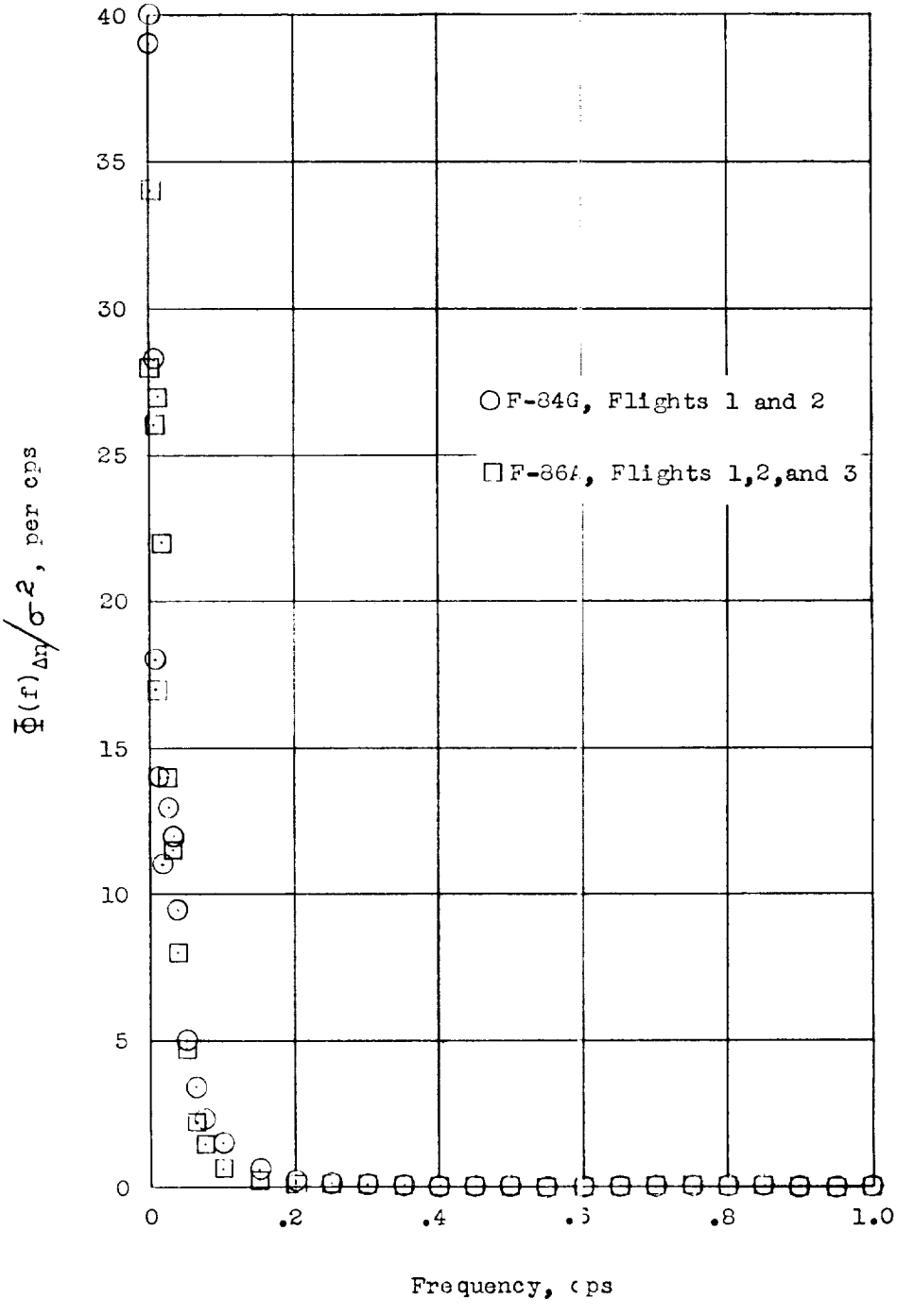

Figure 13.- Comparison of power spectral densities of normal load factor on a linear scale for two operational flights of the F-84G airplane and three operational flights of the F-86A airplane.

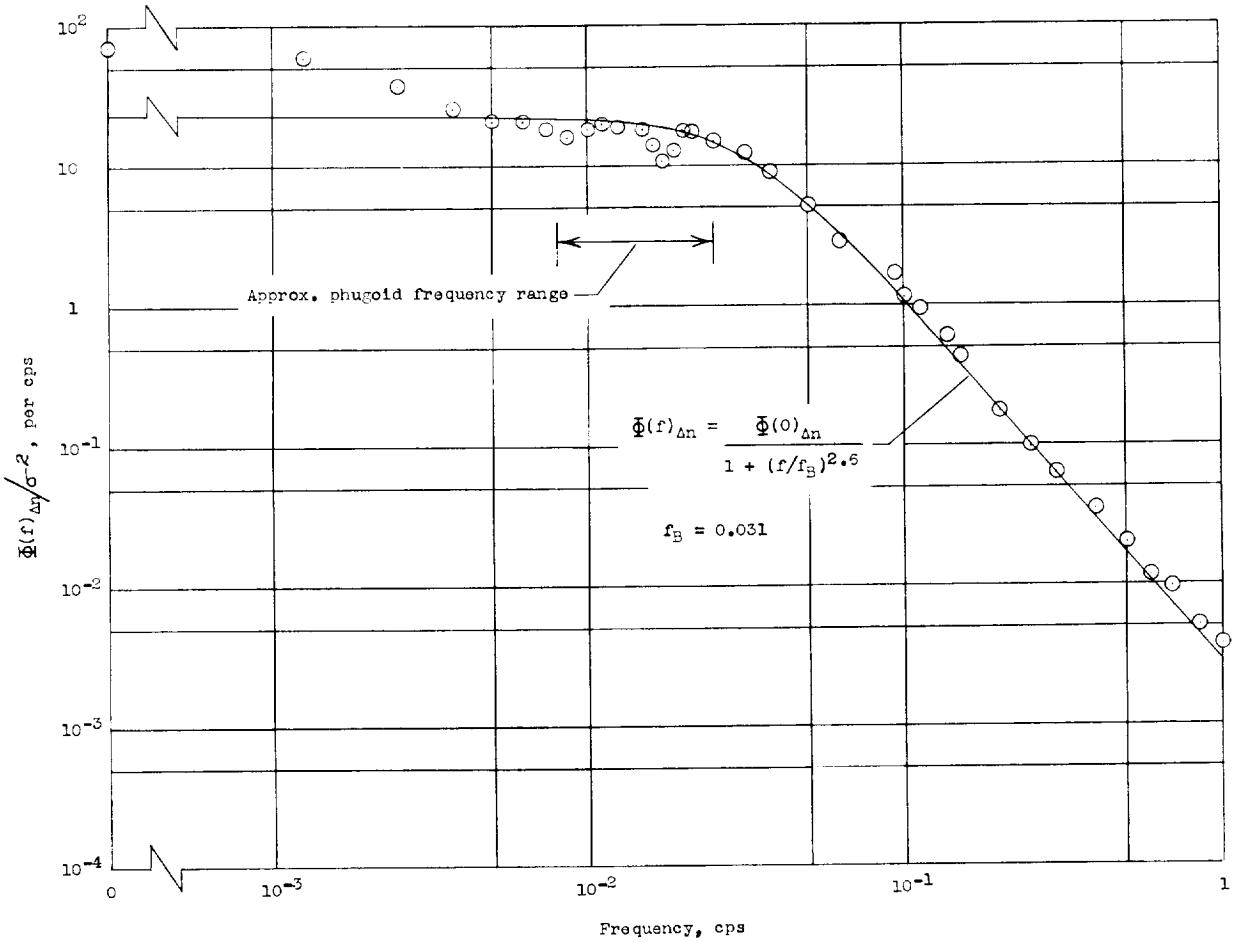

Figure 14.- Comparison of the combined power spectral densities for two operational flights of the F-84G airplane and three operational flights of the F-86A airplane with the analytical spectrum $\Phi(f)_{\Delta n} = \Phi(0)_{\Delta n} / 1 + \left(f/f_B\right)^a$.

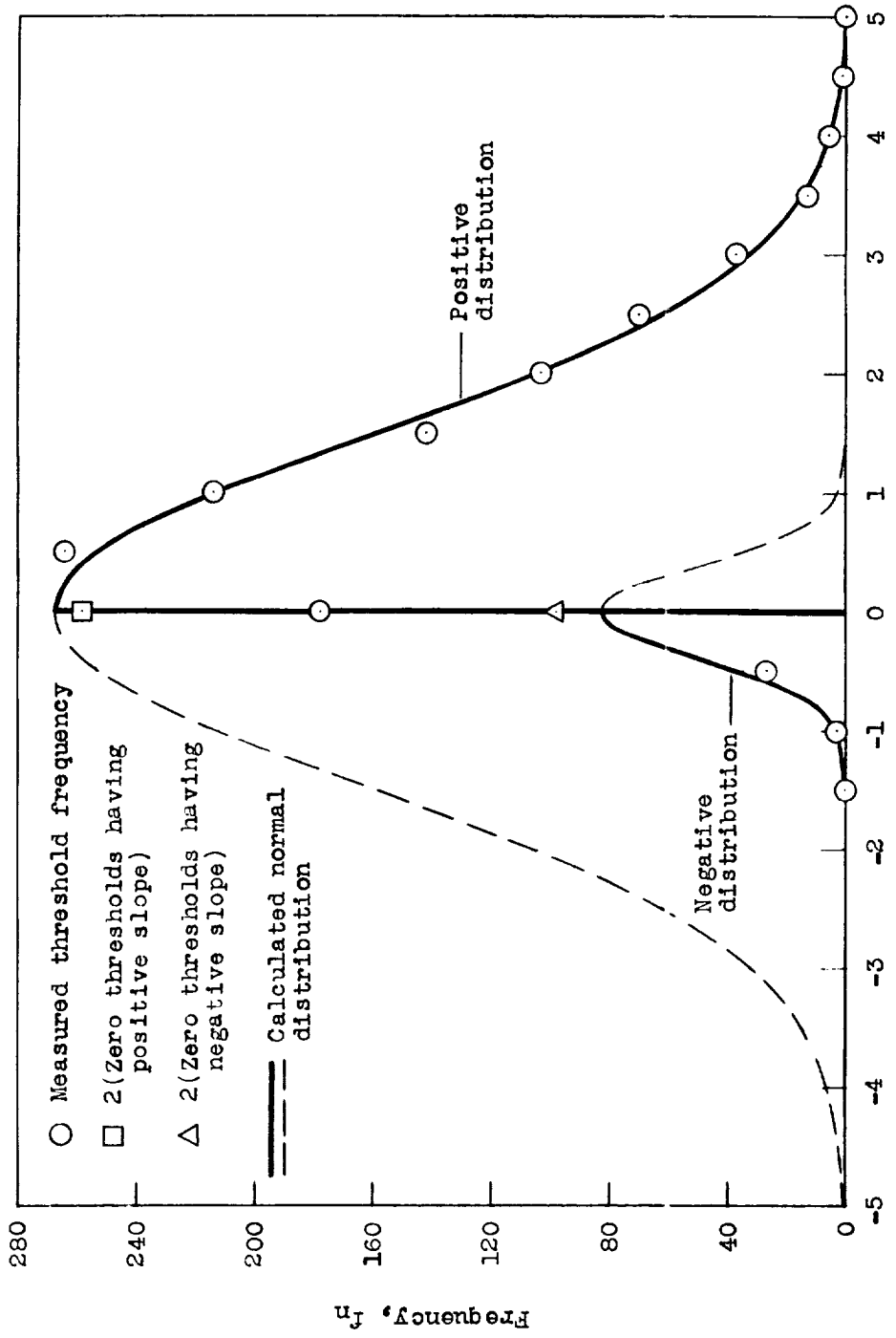

Figure 15.- Illustration of truncated normal distribution used in describing threshold counts of normal load factor for F-86A airplane, flights 1, 2, and 3.

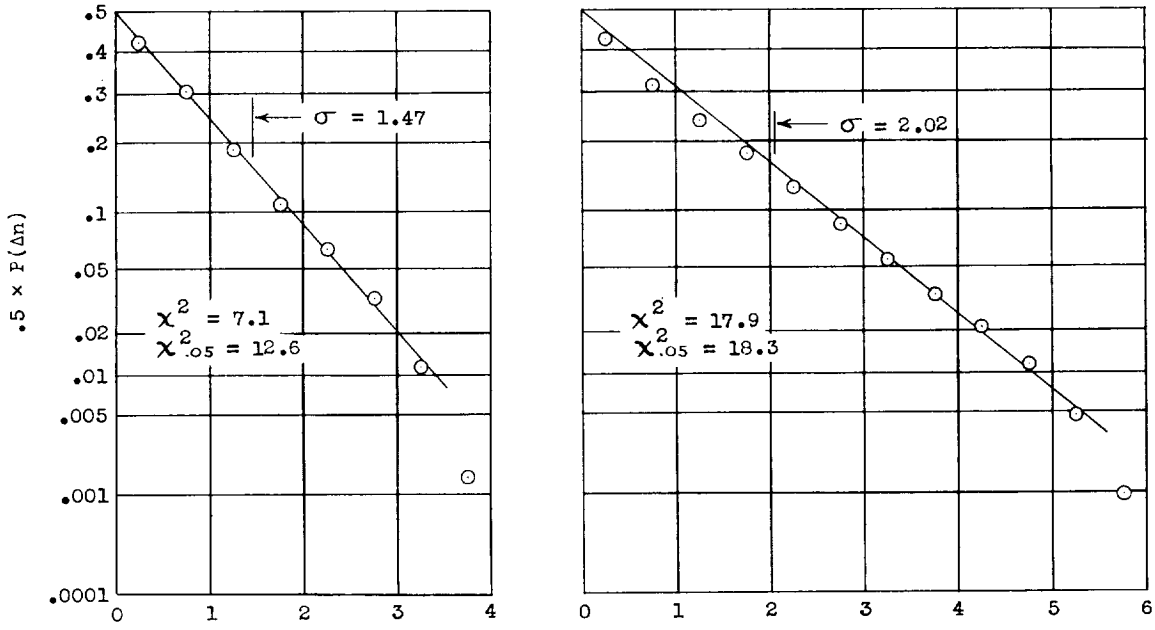

(a) Flight 1.

(b) Flight 2.

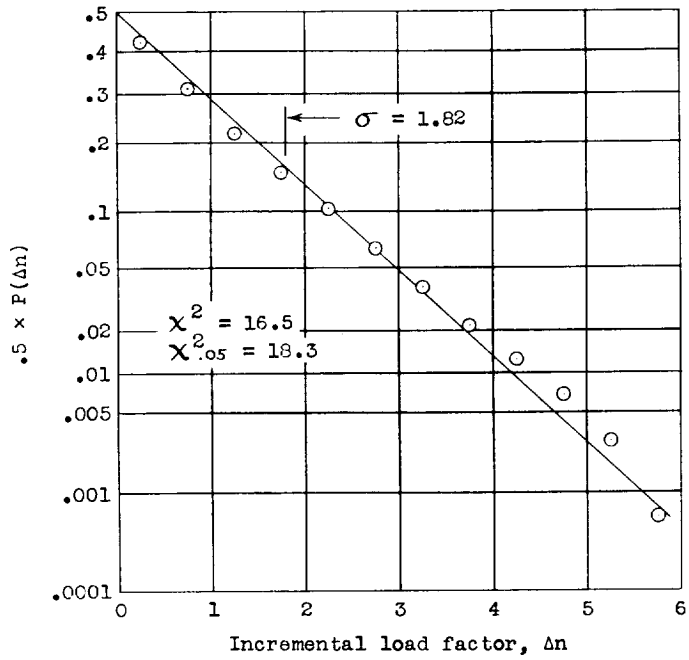

(c) Flights 1 and 2.

Figure 16.- Probability that a given threshold value of load factor will be exceeded. F-84G airplane.

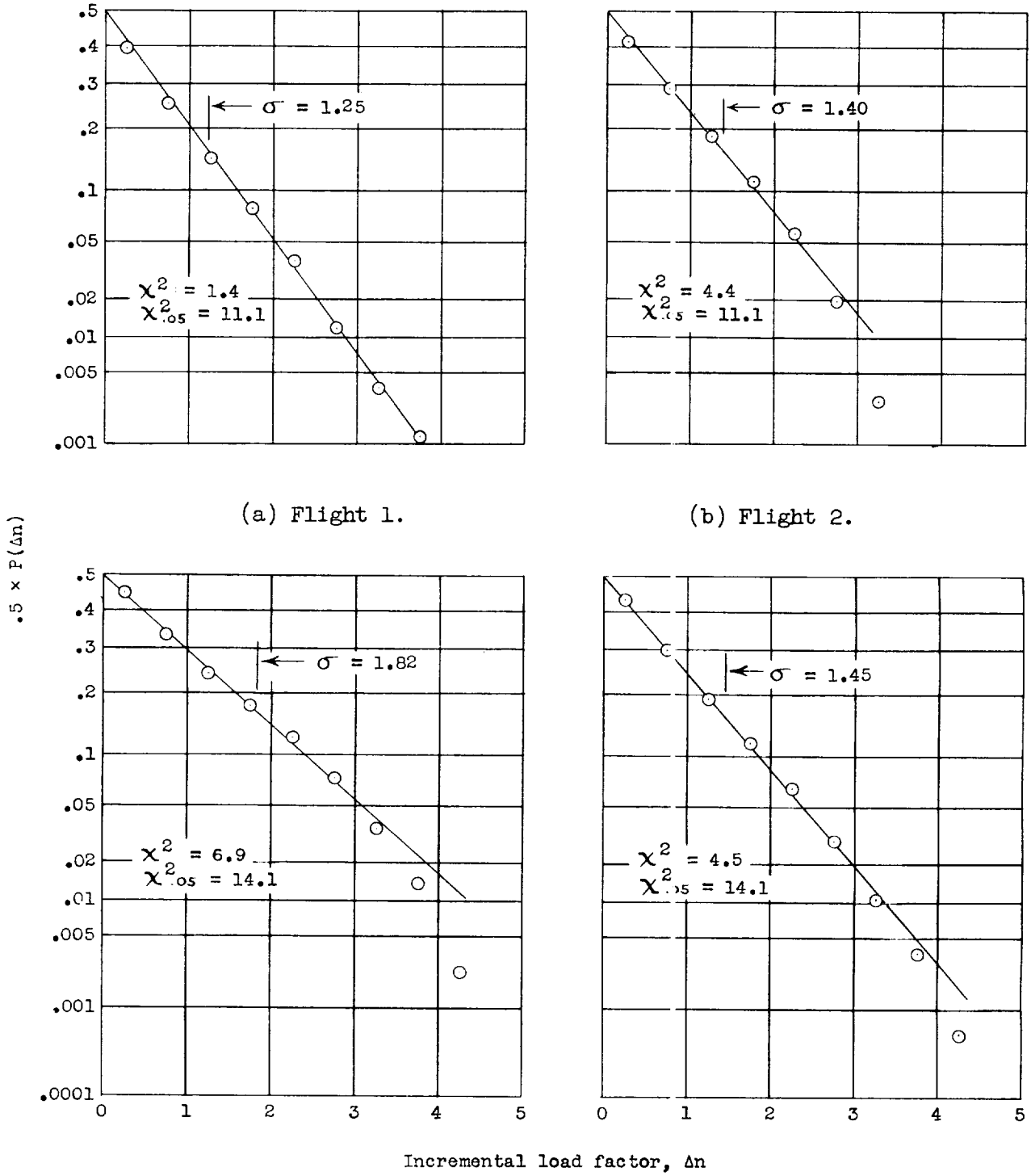

(a) Flight 1.

(b) Flight 2.

(c) Flight 3.

(d) Flights 1, 2, and 3.

Figure 17.- Probability that a given threshold value of load factor will be exceeded. F-86A airplane.

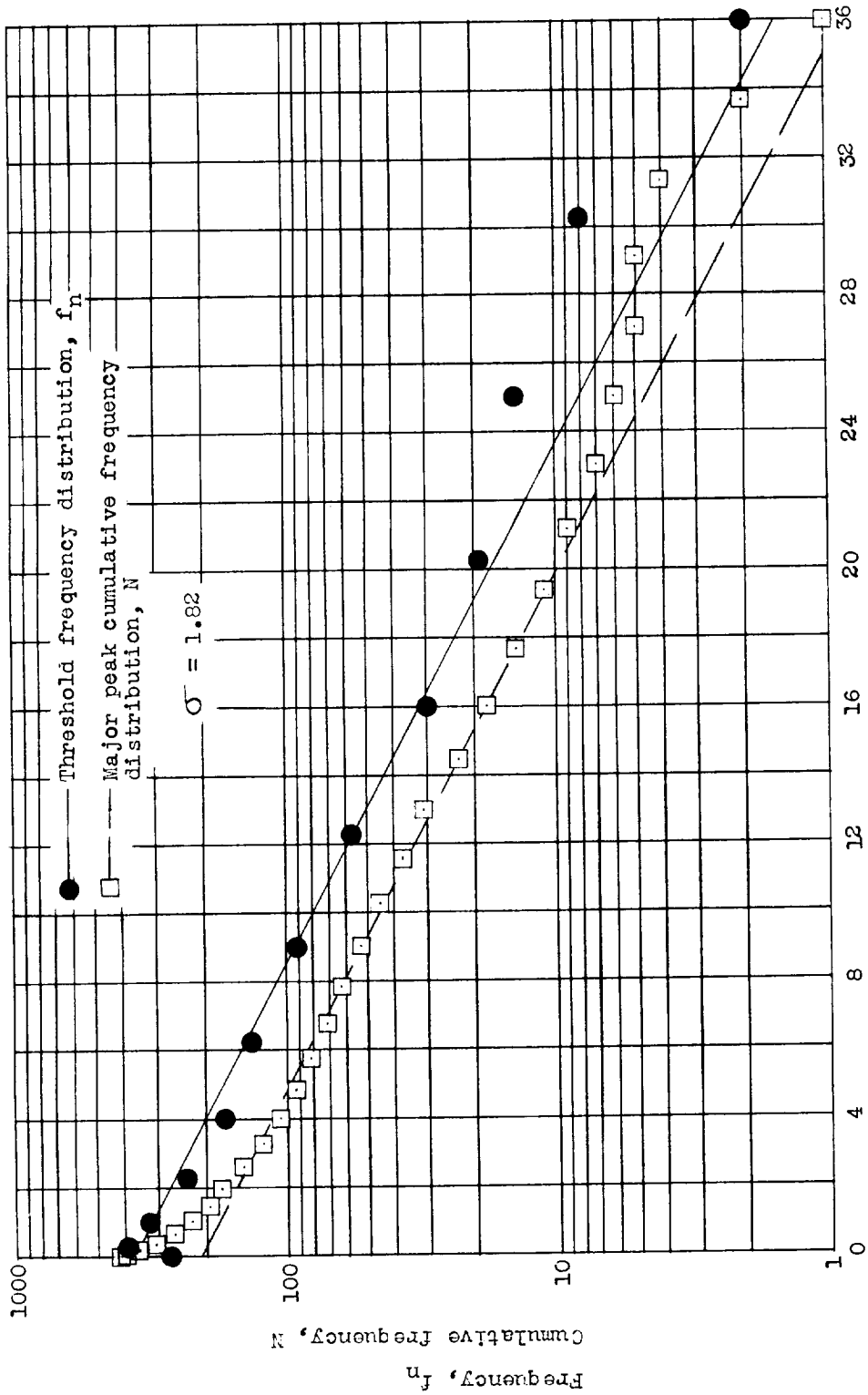

Figure 18.- Distribution of normal load factor threshold counts and major peaks for the F-8HG airplane, flights 1 and 2.

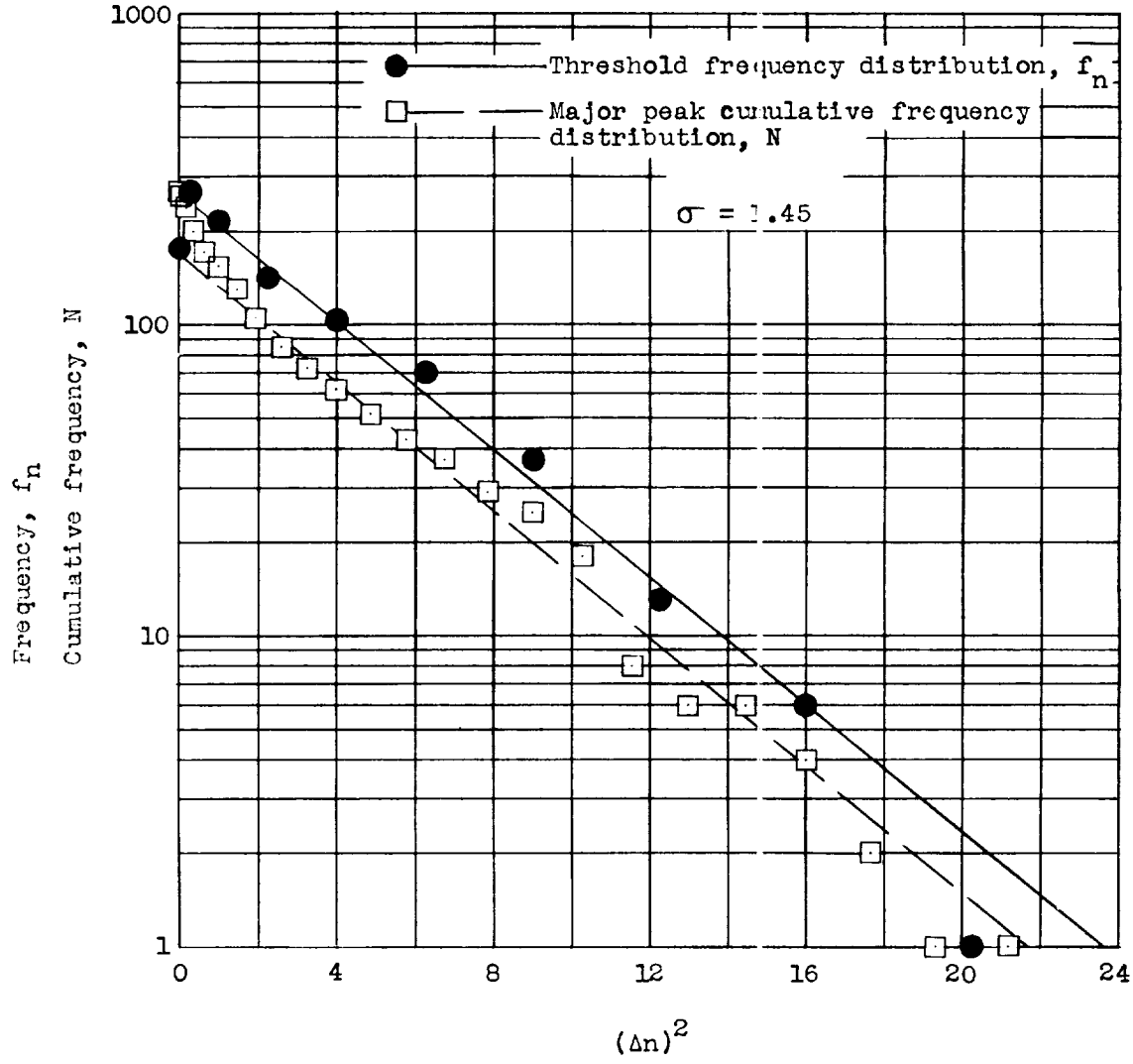

Figure 19.- Distribution of normal load factor threshold counts and major peaks for the F-86A airplane, flights 1, 2, and 3.

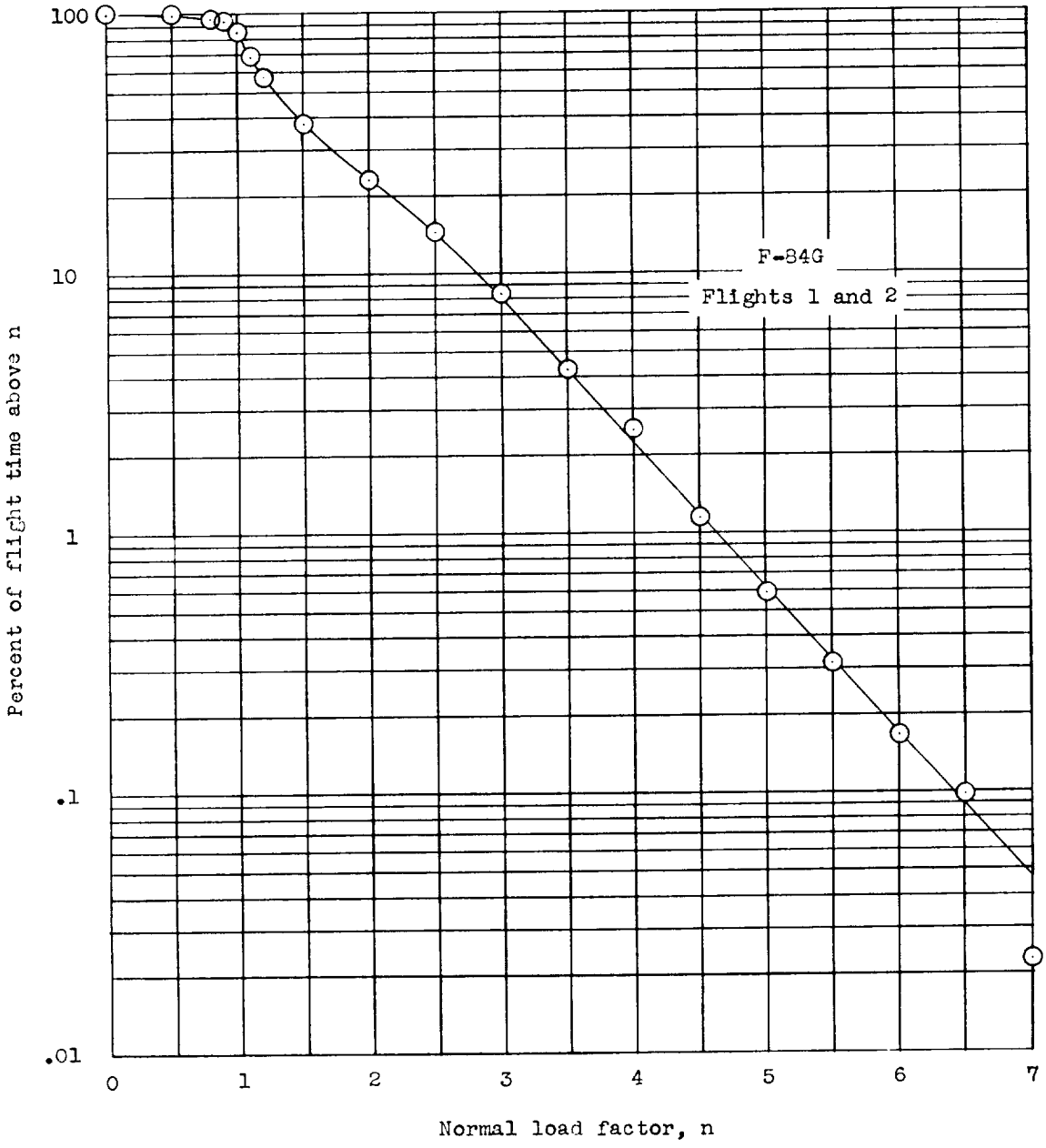

Figure 20.- Amount of flight time spent above given load factors for flights 1 and 2, F-84G airplane.

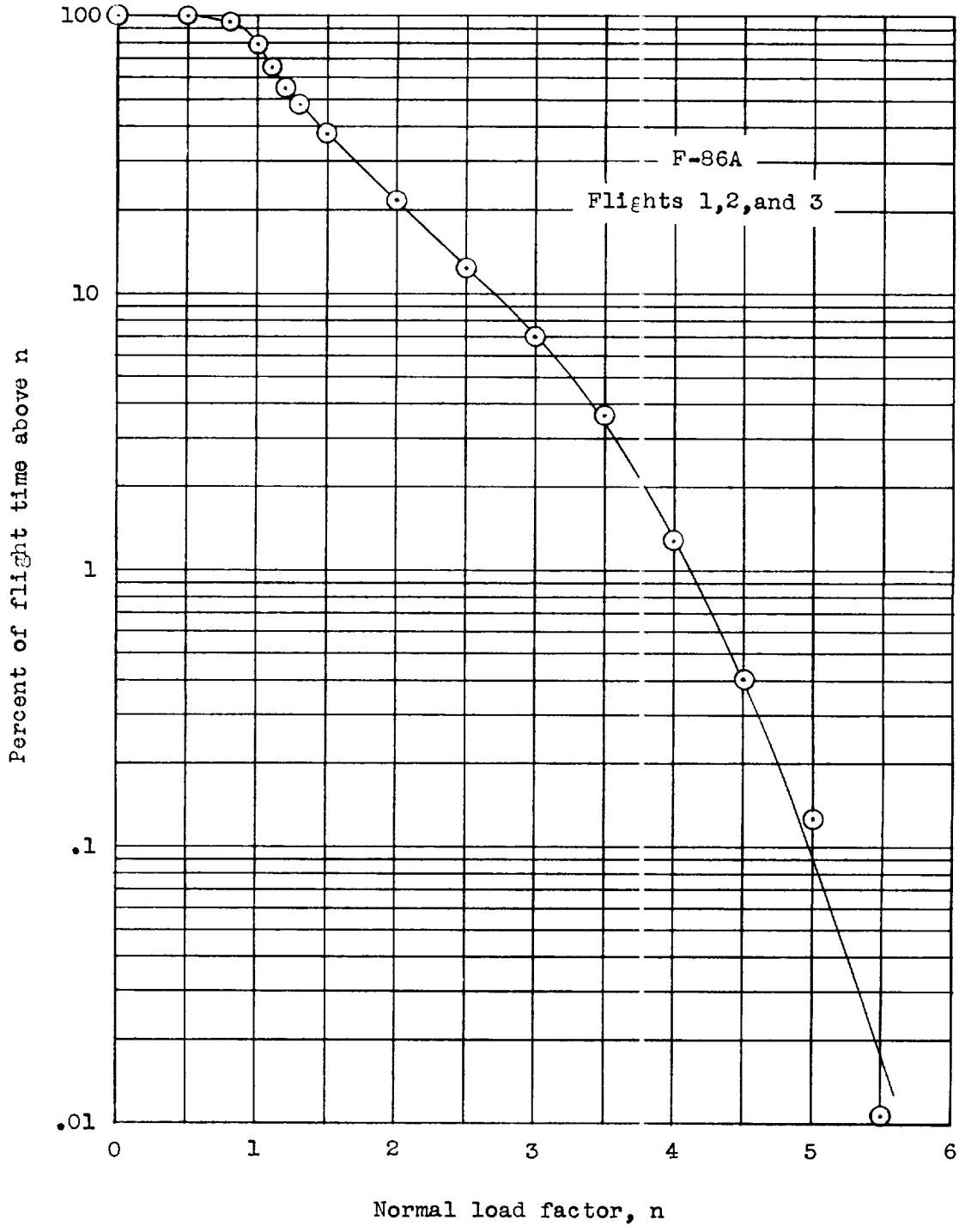

Figure 21.- Amount of flight time spent above given load factors for flights 1, 2, and 3, F-86A airplane.

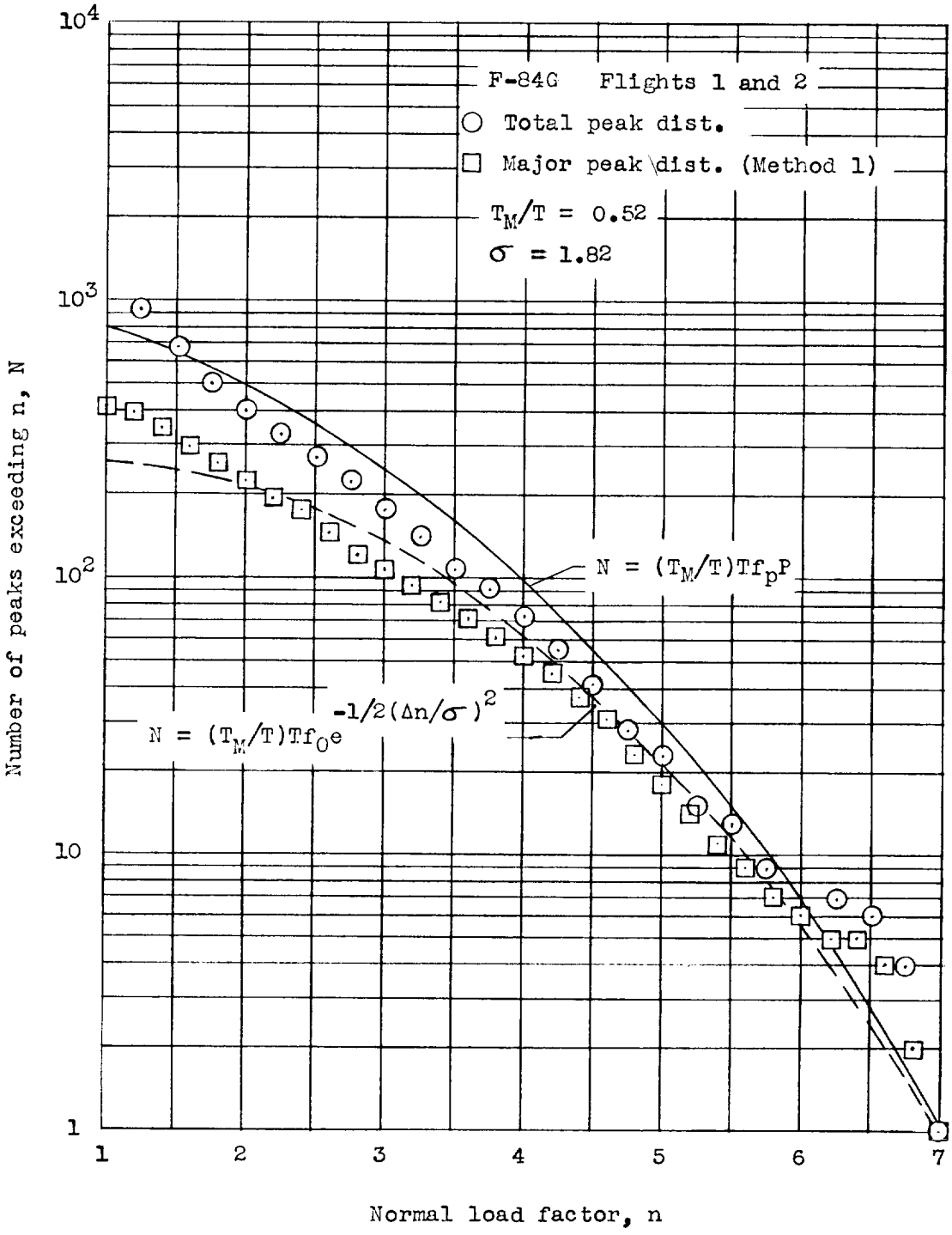

Figure 22.- Comparison of load factor peak distributions with those obtained from power spectral densities. F-84G airplane.

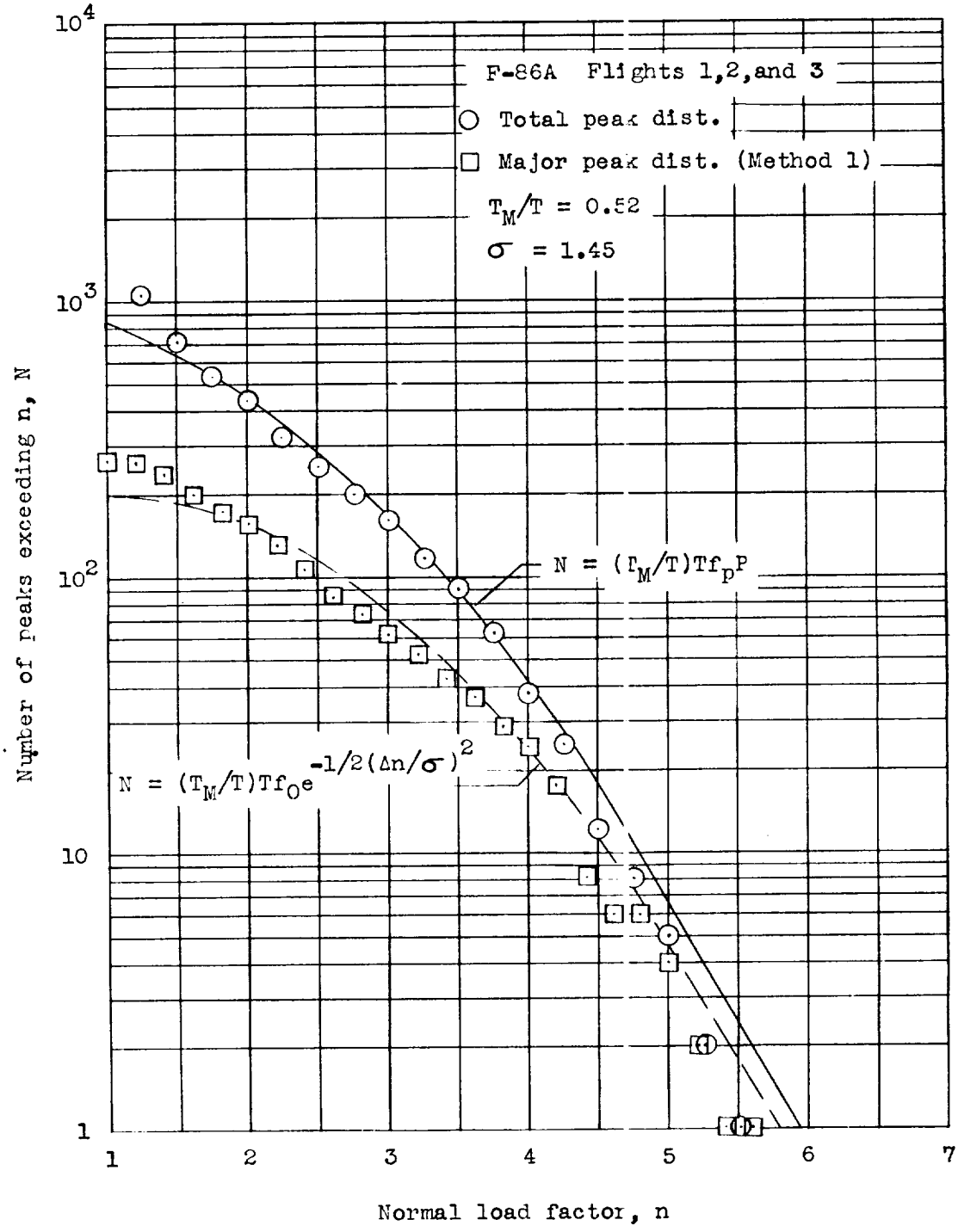

Figure 23.- Comparison of load factor peak distributions with those obtained from power spectral densities. F-86A airplane.

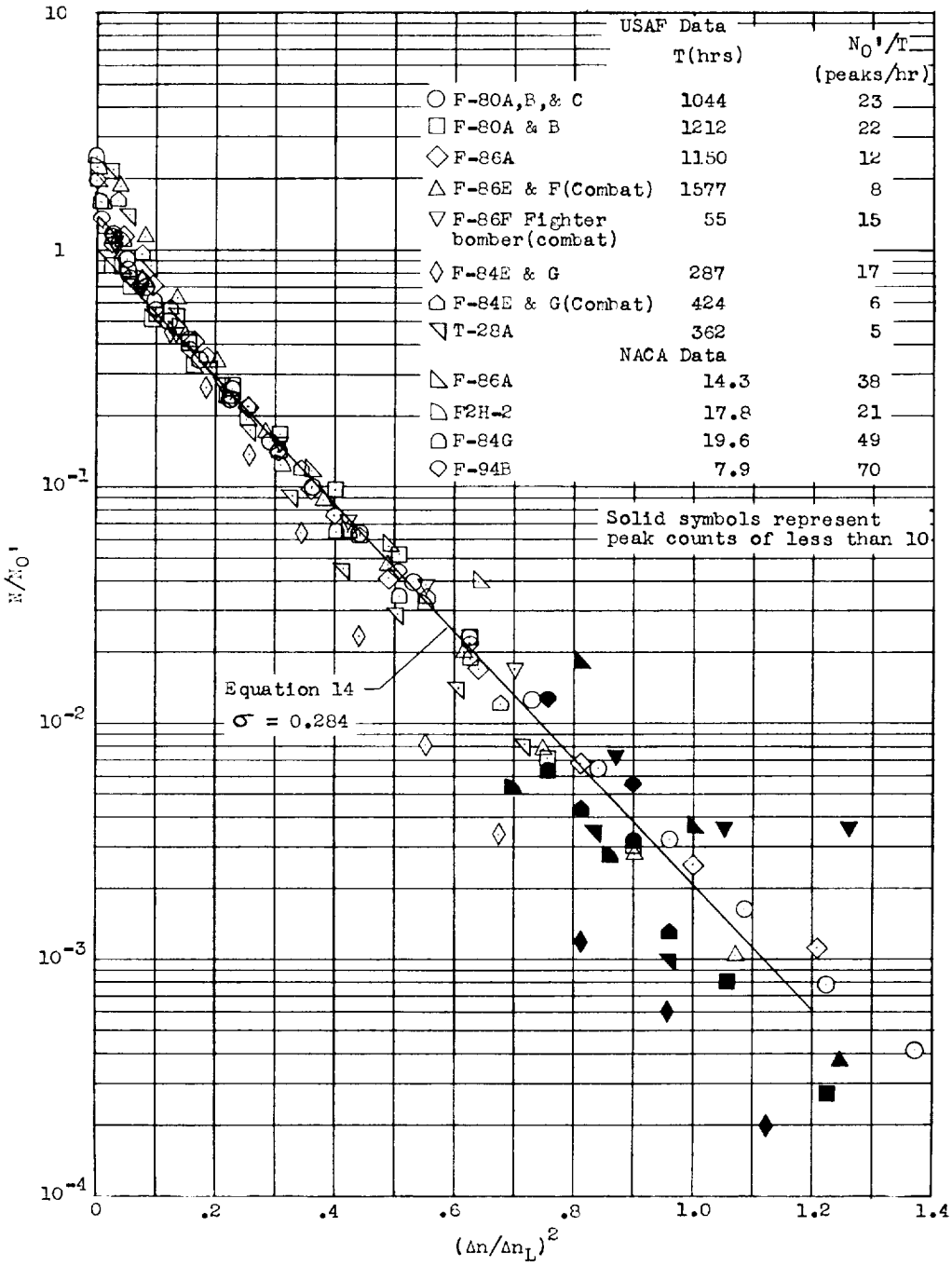

Figure 24.- Percentage of load factor peaks exceeding a given value of $\left(\Delta n/\Delta n_L\right)^2$ obtained in squadron operations for fighter-type airplanes.

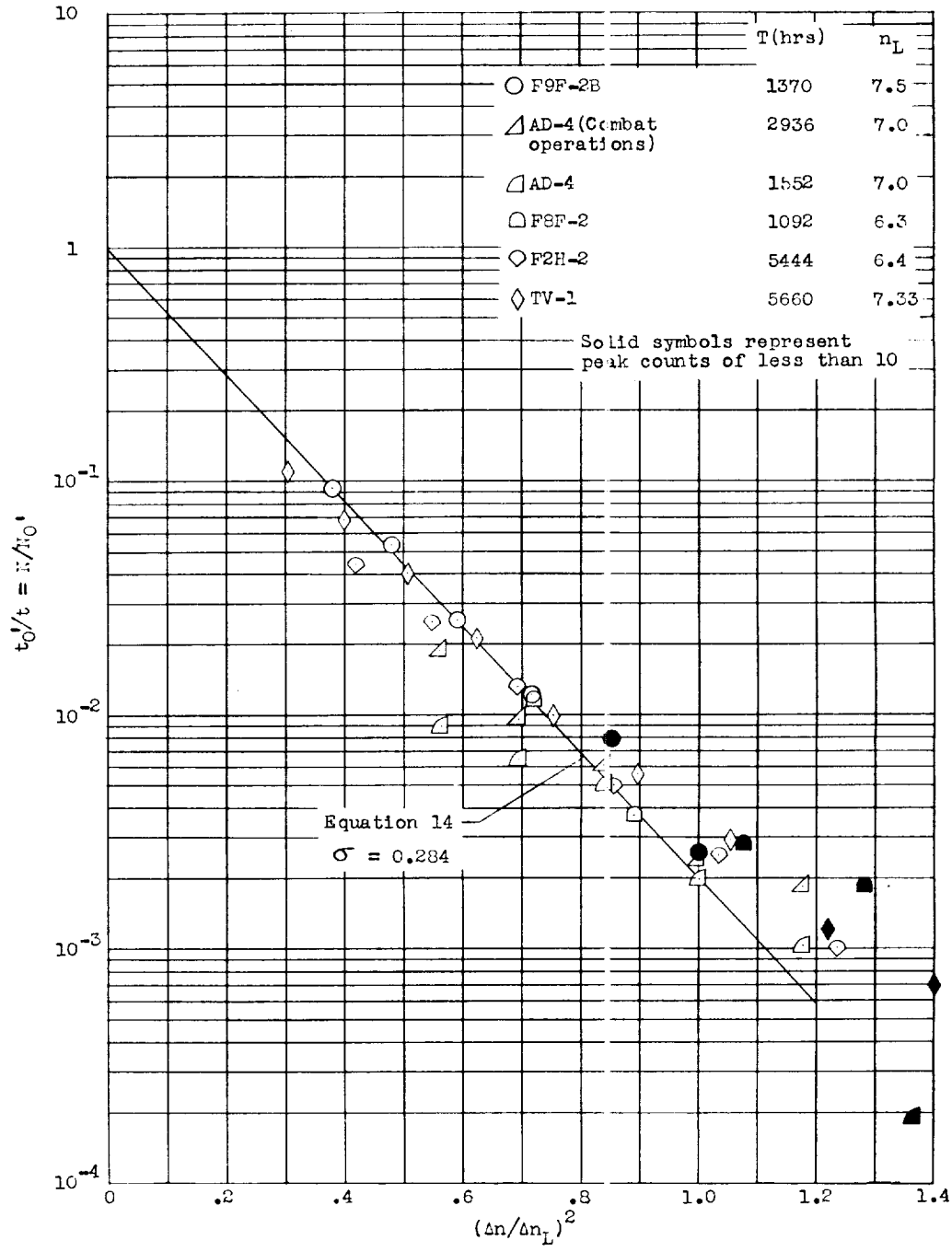

Figure 25.- Percentage of load factor peaks exceeding a given value of $\left(\Delta n/\Delta n_L\right)^2$ obtained from V-g records obtained during squadron operations for fighter-type airplanes.

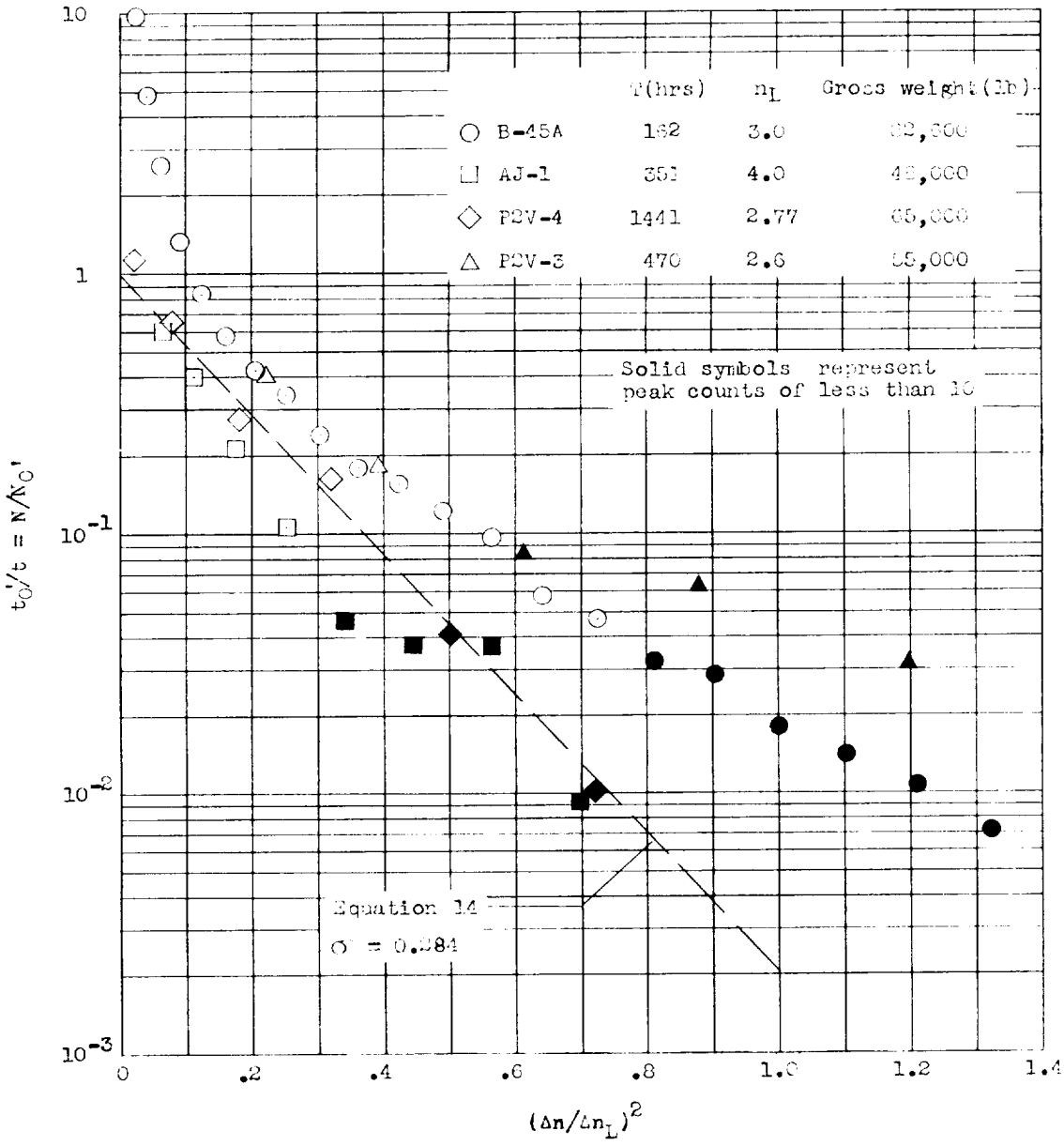

Figure 26.- Percentage of load factor peaks exceeding a given value of $\left(\Delta n/\Delta n_L\right)^2$ obtained in squadron operations for large airplanes.

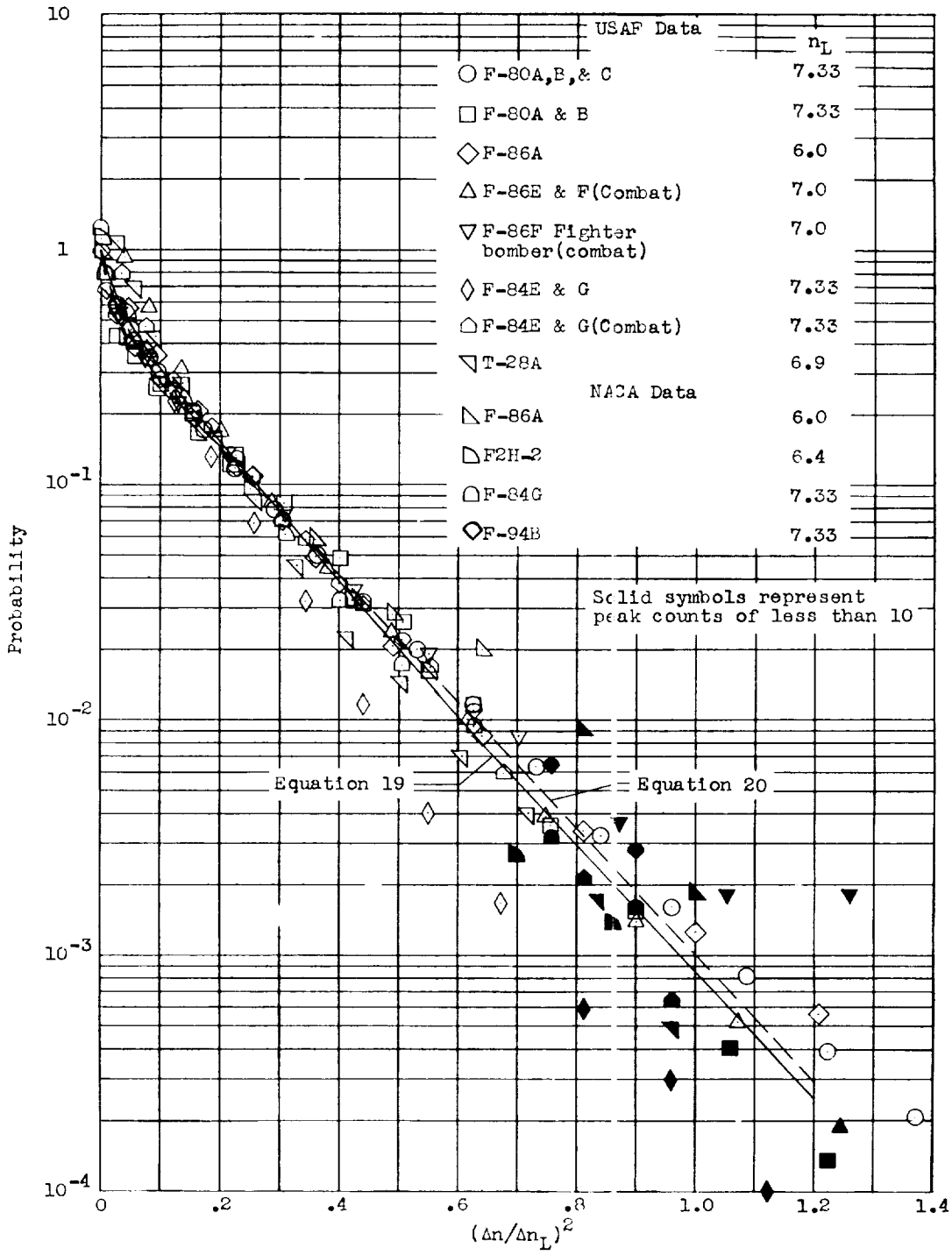

Figure 27.- Comparison of load factor peak cumulative distributions with analytical distributions for fighter-type airplanes.

NASA - Langley Field, Va. L-1557